University of Wisconsin
Madison, Wisconsin

Article

The Evaporation from Drops. Part I & II

Author:
William E. Ranz
1922 – 2009

Author:
W. Robert Marshall,
1916 – 1988

Chemical Engineering Progress,
Volume 48, pp. 141–146, 173–180, 1952

Abstract

An investigation was made of the factors influencing the rate of evaporation of pure liquid drops, and the rate of evaporation of water drops containing dissolved and suspended solids. The study was restricted to a Reynolds number range of 0 to 200, the range usually encountered in spray-drying operations. Independent correlations of heat- and mass- transfer rates were obtained from drop temperature measured with 0.5 mil thermocouples[1]. Drop diameters ranged from 0.06 to 0.11 cm, and air temperatures up to 220 °C.

Results of studies on pure liquid drops confirmed the analogy between heat and mass transfer at low Reynolds numbers, and verified the simple expression for the Nusselt number at zero Reynolds number. A general correlation of existing data on spherical particles showed that the results of this study could be extrapolated with remarkable accuracy five times beyond the experimental range of Reynolds numbers.

Studies on water drops containing dissolved and suspended solids furnished a preliminary insight into the mechanism of the formation of particles dried from drops. The results showed that when the solid was in solution the drop evaporated initially as though it were saturated throughout, even though its average concentration was less than saturation. This was shown to be true for solutions of ammonium nitrate and sodium chloride, and a convenient method for estimating the drop temperature and evaporation rate for this case was proposed. For drops containing insoluble materials, the initial evaporation rate was found to correspond to that for pure water. When the drop formed a solid structure and its diameter became constant, the falling-rate period ensued during which the drop temperature rose continually. This temperature rise was due to both heat of crystallization and sensible heat transfer, in the case of solutions, and primarily to sensible heat transfer in the case of suspensions.

[1]mil = Military Specification according to a validated documentation.

Contents

Notation **7**

1. Introduction **10**

2. Review of Previous Work **11**

3. Theoretical Considerations **12**
3.1. Heat- and Mass-Transfer Equations for an Evaporating Drop 12
3.2. Limiting Condition at Zero Reynolds Number 14
3.3. Forced Convection 14
3.4. Free Convection 15
3.5. Surface Conditions 16
3.6. Effect of Dissolved and Suspended Solids 16

4. Experimental Equipment, Procedures, and Measurements **19**

5. Measurement of Evaporation from Drops in Still Air **24**

6. Transport Properties of Air and Water Vapor **25**

7. Calculation Procedures **27**

8. Experimental Results for Pure Liquid Drops **29**

9. Discussion of Results on Evaporation from Pure Liquid Drops **42**
9.1. Comparison with Other Data 42
9.2. Free Convection 43
9.3. Drop Temperatures 43
9.4. Extrapolation of Results to Higher Air Temperatures 44

10. Evaporation from Drops Containing Solids in Solution and Suspension **46**
10.1. Water Drops Containing Soluble Salts 46
10.2. Drying Drops in Still Dry Air with Heat of Cirystallization and Supersaturation Effects 47
10.3. Formation of Solid Surfaces 49
10.4. Qualitative Picture of Evaporation of a drop Containing Sodium Chloride 52

11. Estimation of Drying Time **53**

12. Acknowledgement **55**

A. Biographical Notes **56**
A.1. William E. Ranz (1922–2009) 56
A.2. W. Robert Marshall (1916–1988) 56

Bibliography **63**

List of Figures

3.1. Temperature exploration around an evaporating water drop 18

4.1. Photograph of experimental equipment 22
4.2. Photomicrograph of an evaporating water drop 23

5.1. Equipment for evaporation of drops in still air 24

6.1. Transport properties of air and water vapor-air mixtures 26

8.1. Heat and mass-transfer correlation for evaporating water drops . . . 33
8.2. Mass-transfer evaporating water drops 34
8.3. Evaporation of water drop in still dry air 36
8.4. Transfer rates in hot dry air 37
8.5. Evaporation rates of aniline drops 37
8.6. Mass-transfer correlation of evaporating benzene drops 41

9.1. Correlation of mass- and heat-transfer rates for single particles . . . 42
9.2. Free convection for spheres 45

10.1. Vapor pressure H_2O over water and saturated aqueous solutions of NH_4NO_3 47
10.2. D_p^2 and ΔT vs. time for drop containing different substances 50
10.2. (Cont.) 51

Notation

A	area of transfer interface
C	heat evolved by crystallization per unit quantity of water evaporated from a saturated solution
C_l	specific heat of liquid drop
C_p	specific heat of gas at constant pressure
C_s	specific heat of particle per unit weight of solid
D_p	diameter of drop
D_{pc}	critical diameter of drop and dried particle
$\mathscr{D}_v$	diffusivity of vapor in air
g	acceleration of gravity
h	rate of heat transfer per unit area of interface per unit temperature difference across the transfer path
h_c	rate of heat transfer by conduction and convection per unit area of interface per unit temperature difference across transfer path
	$r_{Aai}/\Delta p_A$ = rate of mass transfer per unit area of interface per unit partial pressure difference across the transfer path
M	molecular weight of liquid in the drop
$\bar{M}_m$	average molecular weight of gas mixture in the transfer path
Gr	$D_p^3\rho^2 g\beta\Delta T/\mu^2$ = Grashof number
Nu	$h_c\mathscr{D}_v/\kappa$ = Nusselt number
Nu′	$\kappa_G\bar{M}_m D_p p_f/\mathscr{D}_v\rho$ = mass-transfer number analogous to Nusselt number for heat transfer
Pr	$C_p\mu/\kappa$ = Prandtl number
Sc	$\mu/\rho\mathscr{D}_v$ = Schmidt number
Re	$D_p\rho v_0/\mu$ = Reynolds number
P	$\pi/v_0^2\rho$ = dimensionless pressure
p_A	partial pressure of diffusing vapor

p_{Ai}	partial pressure of diffusing vapor at interface
p_{Ao}	partial pressure of diffusing vapor in main gas stream
p_f	average value of $(\pi - p_A)$ across transfer path
p_A	$(p_{Ai} - p_A)/(p_{Ai} - p_{Ao})$ = dimensionless partial pressure
q_{ai}	rate of heat transfer per unit area of interface
R	r/D_p = dimensionless radial distance
r	radial distance from center of drop
r_{Aai}	rate of transfer of diffusing component per unit area of interface
T	Temperature
T_i	temperature at interface
T_o	temperature in main stream
T	$(T - T_i)/(T_o - T_i)$ = dimensionless temperatures; also absolute temperature
T_r	absolute temperature of surroundings for calculating effect of radiation
v	velocity of fluid
v_r	velocity component perpendicular to interface
v_θ	velocity component parallel to interface
v_0	undisturbed velocity of main fluid stream
$\vec{v}$	velocity of fluid as a vector quantity
$\vec{v}'$	velocity of fluid in potential stream outside boundary layer (v_r' and v_θ' are radial and angular components of potential velocity)
$v_{\text{f.c.}}$	velocity due to free convection = $(D_p g \beta \Delta T)^{\frac{1}{2}}$
V_r	v_r/v_0 = dimensionless radial velocity component
V_θ	v_θ/v_0 = dimensionless angular velocity component
W	moisture content, dry basis
K_1, K_2, m, n, p, q	arbitrary constants in correlation equations
β	temperature coefficient of expansion $(= 1/T)$ for gases
δ	thickness of the boundary layer

Δ	difference in value of variable across the transfer path, e.g. $\Delta T = (T_o - T_i)$, $\Delta p_A = (p_{Ai} - p_{Ao})$
κ	thermal conductivity
μ	(dynamic) viscosity of liquid in drop
π	total pressure; also mathematical symbol for 3.1416...
σ	constant in the radiation equation
τ	time
ϵ	emissivity factor in radiation equation
θ	angular coordinate measured from the axis of flow
λ	latent heat of evaporation
ρ	density of the air
ρ_l	density of liquid in drop
ρ_s	weight of solid material per unit volume of particle

ai	per unit area of interface
A	for component A
c	critical moisture content
i	at the interface
o	in the main fluid stream
r	radial component
θ	angular component
1	initial conditions
2	final conditions

1. Introduction

Methods of predicting the evaporation rates of a single drop and the phenomena associated with the evaporation process are of importance in the analysis of chemical engineering operations involving dispersions in gases. Fundamental data on the factors affecting the rate of heat and mass transfer for a spray droplet are important to the operations of spray drying, spray cooling, humidification, spray absorption, spray extraction, combustion, crystallization, dissolution, transfer in fluidized beds, and any other operation where transfer occurs between a continuous phase and a discontinuous phase which appears as spherical particles. The purpose of this paper is to report a fundamental study of evaporation from drops. This study was divided into the following parts:

1. Rate of heat transfer to the drop surface.
2. Rate of evaporation and mass transfer from the drop surface.
3. Temperature and concentration at the drop surface during evaporation.
4. Effect on evaporation rate of original drop temperature, heats of solution and crystallization, and the way in which solid surfaces form.

Application of the results has been made with specific reference to spray drying. In spray drying, as in most drying problems, the first period of drying, usually termed the constant-rate period, is susceptible to a simple analysis. However, as soon as a spray droplet concentrates to the point where it no longer presents a free liquid surface to the gas stream, it becomes a particle with drying characteristics determined by the nature of the solid structure. The particle then enters a period in which the rate of drying decreases with decreasing moisture content. For applications to the operation of spray drying, this study was primarily concerned with the constant-rate period.

2. Review of Previous Work

Only a small amount of experimental work has been done on the fundamentals of heat and mass transfer in the evaporation of single drops. Experimental difficulties are evident when it is realized that drop diameters should be in the range of 200 µm to 800 µm, and the Reynolds number range should be from 0 to 100 to approach conditions of commercial interest.

KRAMERS, [20] recorded heat-transfer data for spheres in the low Reynolds number range. However, the diameters of the spheres he used were of the order of 1 cm, and free convection obscured the true effect of the velocity of the fluid stream. Meyer, [26], presented an analysis of data on free convection from spheres in quiescent fluids of various kinds.

Evaporation of solid and liquid drops in still air has been treated from the standpoint of simple mass transfer. Experimental data of MORSE, [27], on the sublimation of iodine beads led to a calculation by LANGMUIR, [21] of the diffusivity of iodine vapor in air. FUCHS, [11] presented a theoretical treatment of mass transfer for evaporation of drops in still air. Evaporation of droplets at finite air velocities was treated theoretically and experimentally by FRÖSSLING, [10], but the results were based largely on the evaporation of materials of low volatility so that the problem was essentially one of mass transfer only. FRÖSSLING's data along with other literature data were reviewed by WILLIAMS, [29], who was primarily interested in the evaporation of mustard gas, a substance of low volatility.

As far as the evaporation of drops containing dissolved and suspended solids is concerned, the available data, [37], are meager and inconclusive, and offer no basis for the prediction and explanation of phenomena associated with the constant-rate period. For the falling-rate period only the studies of VAN KREVELIN, [31], on the drying of single particles seem applicable.

3. Theoretical Considerations

The evaporation of a liquid drop is essentially an operation in which heat for evaporation is transferred by conduction and convection from hot gases to the drop surface from which vapor is transferred by diffusion and convection back into the gas stream. The rate of transfer per unit area of interface is a function of the temperature, humidity, and transport properties of the gas, and the diameter, temperature, and relative velocity of the drop.
Boundary layer theory predicts that the rate of transfer is a maximum on the front side of the drop facing the oncoming air stream, decreases to a minimum value near the separation point, and increases to another, but lower, maximum rate on the trailing face which experiences velocities in the reverse direction. Such a distribution of mass transfer rates was shown by FRÖSSLING, [10], for the sublimation of a naphthalene bead.
Figure 3.1 shows a temperature difference exploration around an evaporating water drop. It is evident that the rate of heat transfer will be largest on the side facing the air stream where the temperature gradient is steepest and the isotherms are close together. This temperature exploration reveals the significant fact that the thickness of the boundary layer is, in general, of the same order of magnitude as the diameter of the evaporating water drop. Thus, any theoretical development or empirical correlation should account for the variable cross-sectional area of transfer through the boundary layer.

3.1. Heat- and Mass-Transfer Equations for an Evaporating Drop

From FRÖSSLING's boundary layer equations for a blunt-nosed body of revolution, [10], and from equations for heat and mass transfer, a set of four dimensionless coupled partial differential equations can be developed for the evaporation of a liquid drop in an air stream. These may be written in dimensionless quantities as

follows:

$$\left(\frac{1}{\mathrm{Pr}\,\mathrm{Re}}\right)\cdot\left\{\frac{1}{R^2}\cdot\frac{\partial}{\partial R}\left(R^2\frac{\partial T}{\partial R}\right)+\frac{1}{R^2\cdot\sin\theta}\cdot\frac{\partial}{\partial R}\left(\sin\theta\frac{\partial T}{\partial\theta}\right)\right\}$$
$$=V_r\cdot\frac{\partial T}{\partial R}+V_\theta\cdot\frac{\partial T}{\partial\theta} \tag{3.1}$$
(Heat balance)

$$\left(\frac{\pi}{\mathrm{Sc}\,\mathrm{Re}\,p_f}\right)\cdot\left\{\frac{1}{R^2}\cdot\frac{\partial}{\partial R}\left(R^2\frac{\partial P_A}{\partial R}\right)+\frac{1}{R^2\cdot\sin\theta}\cdot\frac{\partial}{\partial\theta}\left(\sin\theta\frac{\partial P_A}{\partial\theta}\right)\right\}$$
$$=V_r\cdot\frac{\partial P_A}{\partial R}+V_\theta\cdot\frac{\partial P_A}{\partial\theta} \tag{3.2}$$
(Mass balance on component A)

$$\frac{V_\theta}{R}\cdot\frac{\partial V_\theta}{\partial\theta}+V_r\cdot\frac{\partial V_\theta}{\partial R}=-\frac{1}{R}\cdot\frac{\partial P}{\partial\theta}+\frac{1}{\mathrm{Re}}\cdot\frac{\partial^2 V_\theta}{\partial R^2} \tag{3.3}$$
(Force balance–modified Navier-Stokes equation)

$$\frac{1}{R}\cdot\frac{\partial}{\partial\theta}\left(R\cdot\sin\theta V_\theta\right)+\frac{\partial}{\partial R}\left(R\cdot\sin\theta V_r\right)=0 \tag{3.4}$$
(Equation of continuity)

with boundary conditions:

$$(1)\qquad T=P_A=0\,, \tag{3.5a}$$
$$V_\theta=V_r=0\,,\quad\text{at}\quad R=\frac{1}{2} \tag{3.5b}$$
$$(2)\qquad T=P_A=1.0\,,\quad\text{at}\quad R=\infty\,; \tag{3.5c}$$
$$V_\theta=\frac{v'_\theta}{v_0}\,; \tag{3.5d}$$
$$V_r=\frac{v'_r}{v_0}\,,\quad\text{at}\quad R>\frac{\delta}{D_p} \tag{3.5e}$$

where δ is the thickness of the boundary layer. Mathematically the boundary layer is defined as the region of velocities whose magnitudes are less than those for potential flow because of the retarding effect of friction at the interface.
A general solution of this formidable set of equations is not possible, and such a solution is not justified in view of the numerous assumptions which must be

made regarding average physical properties across the transfer path, and in view of the existence of drop rotation, drop vibration, and unsteady-state phenomena. However, the heat- and mass-transfer numbers can be shown to take the theoretical and functional form

$$\begin{aligned} \mathrm{Nu} = -\frac{1}{2} \cdot \int_0^{\pi} \left(\frac{\partial T}{\partial R} \right)_{R=\frac{1}{2}} \sin\theta \, \mathrm{d}\theta &= \mathrm{Nu}(\mathrm{Re}\,, (\mathrm{Re}\,\mathrm{Pr})) \\ &= \mathrm{Nu}'(\mathrm{Re}\,, (\mathrm{Re}\,\mathrm{Pr})) \end{aligned} \tag{3.6}$$

$$\begin{aligned} \mathrm{Nu}' = -\frac{1}{2} \cdot \int_0^{\pi} \left(\frac{\partial P_A}{\partial R} \right)_{R=\frac{1}{2}} \sin\theta \, \mathrm{d}\theta &= \mathrm{Nu}'(\mathrm{Re}\,, (\mathrm{Re}\,\mathrm{Sc}\,\frac{p_f}{\pi})) \\ &= \mathrm{Nu}(\mathrm{Re}\,, (\mathrm{Re}\,\mathrm{Sc}\,\frac{p_f}{\pi}))\,. \end{aligned} \tag{3.7}$$

The analogy shown by Equations Equation 3.6 and Equation 3.7 arises from the fact that Equations Equation 3.1 and Equation 3.2 are mathematically equivalent and subject to the same boundary conditions. Thus, Nu and Nu′ should have exactly the same functional form where Pr for heat transfer is equivalent to $\mathrm{Sc}\,\frac{p_f}{\pi}$ for mass-transfer. This is an important conclusion, applicable to all heat- and mass-transfer problems where the rate of transfer is controlled by the boundary layer.
Since $\frac{p_f}{\pi}$ is nearly unity in most applications, it is omitted as a factor on Sc in the material which follows and is implied only as a correction in broad extrapolations of recommended results.

3.2. Limiting Condition at Zero Reynolds Number

Since the physical situation in finely dispersed systems is such that the relative velocity and Re become vanishingly small, the limiting case for a drop evaporating in still air is of practical importance. For $v_\theta = v_r = 0$, Equation 3.1, Equation 3.2, Equation 3.6, and Equation 3.7 give the relationship

$$\mathrm{Nu} = \mathrm{Nu}' = 2.0 \tag{3.8}$$

From Equation 3.8 it can be shown that the rate of change of surface area of a pure liquid drop is constant during evaporation and that the total lifetime of such a drop is proportional to the square of the original drop diameter, facts reported empirically and theoretically by many investigators, [10], [11], [21], [29].

3.3. Forced Convection

For finite velocities several solutions based on simplifying assumptions have been proposed. Johnstone and Kleinschmidt, [16], in an absorption study postulated

a hypothetical tube of gas, described by the trace of the periphery of a liquid particle in motion through a gas, whose thickness is equal to the distance heat and/or mass can be transferred in the time it takes the particle to move through one diameter. JOHNSTONE, PIGFORD and CHAPIN, [17], [18] developed a solution of the BOUSSINESQ type for heat transfer. These simplified solutions failed to give a finite value of 2.0 for Re = 0. To obtain the proper limiting value of Nu = 2.0 at Re = 0, JOHNSTONE, PIGFORD and CHAPIN, [17], [18], developed a solution to Equation 3.1 and Equation 3.6 on the assumption that $V_\theta = 1.0$ and $V_r = 0$ at all $R > \frac{1}{2}$.
Experimental data on mass-transfer rates for spheres may be correlated by an empirical equation of the form used by FRÖSSLING, [10]:

$$\mathrm{Nu}' = 2.0 + K_1(\mathrm{Sc})^m \cdot (\mathrm{Re})^n \tag{3.9}$$

where K_1 is a constant, $m = \frac{1}{3}$ and $n = \frac{1}{2}$. By analogy heat-transfer data should be correlated by a corresponding equation:

$$\mathrm{Nu} = 2.0 + K_2(\mathrm{Pr})^p \cdot (\mathrm{Re})^q \tag{3.10}$$

where

$$K_1 = K_2\,,$$
$$p = m = \frac{1}{3}$$

and

$$q = n = \frac{1}{2}\,.$$

Equation 3.9 and Equation 3.10 are both consistent with the theoretical requirement that $\mathrm{Nu} = \mathrm{Nu}' = 2$ at Re = 0. At high values of Re, the constant term becomes less significant, so that Equation 3.9 and Equation 3.10 may be converted to the familiar j-factor equations of CHILTON and COLBURN, [4], [5].

3.4. Free Convection

At zero relative velocity, if heat transfer is by simple conduction and mass transfer is by simple diffusion, $\mathrm{Nu} = \mathrm{Nu}' = 2.0$. In the practical case, however, a density difference exists across the transfer path, and a fluid velocity caused by free convection contributes to the transfer rate. To account for this effect, it is proposed that the velocity term in Re, be taken as $|\vec{v}_0 + \vec{v}_{\mathrm{f.c.}}|$, where $\vec{v}_{f.c.}$ is a velocity component due to free convection parallel to gravity. I£ $\vec{v}_{\mathrm{f.c.}}$ is taken equal

$\sqrt{D_p g \beta \Delta T}$, Equation 3.9 and Equation 3.10 for $v_0 = 0$ become

$$\mathrm{Nu}' = 2.0 + K_1(\mathrm{Sc})^{\frac{1}{3}}(\mathrm{Gr})^{\frac{1}{4}} \tag{3.11}$$

$$\mathrm{Nu} = 2.0 + K_2(\mathrm{Pr})^{\frac{1}{3}}(\mathrm{Gr})^{\frac{1}{4}} \tag{3.12}$$

These are consistent with standard empirical correlations for free convection, [25], at least insofar as the functional form of Gr, is concerned.

3.5. Surface Conditions

In order to calculate evaporation rates, surface temperatures, T_i and/or surface partial pressures, p_{Ai}, must be known. To estimate T_i and p_{Ai}, a simultaneous graphical solution of two equations must be made. One of these equations is the temperature vapor-pressure relationship, and the other equation is a balance between the rate of heat and mass transfer. These equations may be written as follows:

$$p_{Ai} = p_{Ai}(T_i) \tag{3.13}$$

and

$$\frac{\kappa \Delta T \,\mathrm{Nu}(\mathrm{Re},\mathrm{Pr})}{D_p + \sigma\epsilon \cdot (T_r^4 - T_i^4)} = \frac{\lambda_i \mathscr{D}_v \rho \Delta p_A \,\mathrm{Nu}'(\mathrm{Re},\mathrm{Sc})}{\bar{M}_m D_p p_f} \tag{3.14}$$

where Equation 3.14 equates the heat transferred by conduction, convection, and radiation to the latent heat of evaporation. Either side of the equation may be used to represent the evaporation rate.
For simultaneous heat and mass transfer under conditions of large temperature and concentration driving forces, corrections for sensible heat carried by the vapor molecules and diffusion due to thermal gradients must be taken into account, [6]. Such effects were negligible in this study.

3.6. Effect of Dissolved and Suspended Solids

When a droplet contains dissolved materials which lower the normal vapor pressure of the liquid, p_{Ai} is not only a function of T_i, but also a function of the concentration of the non-volatile component in the surface liquid. The net result is to lower ΔT and Δp_A, such that the evaporation rate becomes lower than that for pure drops of the same size. This effect would not be expected for solutions or suspensions of inert materials; and drops containing such materials can be treated as evaporating at the same rate as pure drops of the same size.
When the normal vapor pressure of the liquid is lowered by dissolved solids, it can be assumed that the drop evaporates at any average concentration as though it were saturated throughout. Hence partial pressure for saturated solutions can be used in Equation 3.13. This simplification is based on the fact that diffusion

coefficients in water are on the order of $1 \times 10^{-5}\,\mathrm{cm^2\,s^{-1}}$, so small that solids will concentrate in the surface by evaporation much faster than they can diffuse toward the center of the drop.
If the heat evolved by crystallization is significant in comparison with the latent heat of evaporation, then the constant-rate period must be treated as two separate periods with a different surface temperature for each period. The first period can be treated as before. In the second period during crystallization, T_i must be calculated from an energy balance which includes the heat of crystallization. This heat contributes to evaporation and increases T_i. Although ΔT is smaller, the rate of evaporation is lower since the total amount of heat being supplied for evaporation is larger and p_{Ai} has increased. From a treatment analogous to that of Williams and Schmitt, [33], a heat balance gives

$$\frac{\lambda_i \mathscr{D}_v \rho \Delta p_A \,\mathrm{Nu}'(\mathrm{Re},\mathrm{Sc})}{\bar{M}_m D_p p_f} = \frac{\kappa \Delta T \,\mathrm{Nu}(\mathrm{Re},\mathrm{Pr})}{D_p} + \frac{C \mathscr{D}_v \rho \Delta p_A \,\mathrm{Nu}'(\mathrm{Re},\mathrm{Sc})}{D_p \bar{M}_m p_f} \tag{3.15}$$

where the effect of radiation is neglected and C is the heat evolved by crystallization per unit quantity of water evaporated from a saturated solution.
Since Nu is nearly equal in value to Nu′ for water vapor in air, the ratio of vapor pressure difference to temperature difference for crystallizing aqueous solutions becomes

$$\frac{\Delta p_A}{\Delta T} = -\frac{\kappa \bar{M}_m p_f}{(\lambda_i - C) \cdot \mathscr{D}_v \rho} \tag{3.16}$$

Thus, if C is significant, the slope of the wet-bulb line, given by Equation 3.16, is increased; and the temperature T_i, where it crosses the curve for the vapor pressure over a saturated salt solution, is also increased.

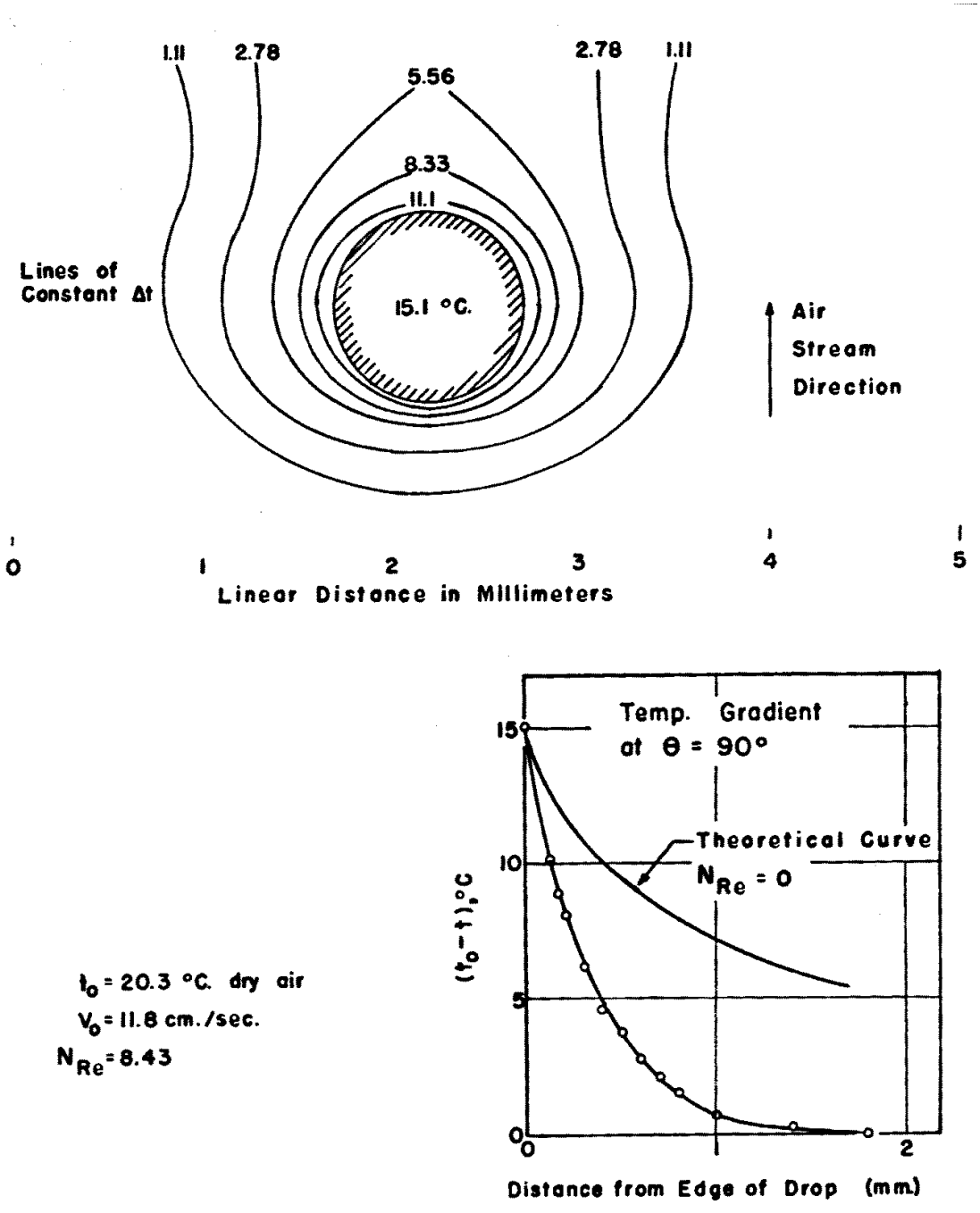

Figure 3.1.: Temperature exploration around an evaporating water drop

4. Experimental Equipment, Procedures, and Measurements

Rates of evaporation and heat transfer were obtained by a microtechnique in which drops of about one millimeter diameter were suspended from a microburette in a vertical, upward-flowing stream of air. Evaporation rates were determined by measuring the rate of feed through the burette necessary to maintain a constant-drop diameter. The temperature of the drop and the air stream were measured with small thermoelements. Evaporation rates in still air were determined in a special dryer. Suspended drops with decreasing diameters were evaporated in hot air streams and in still air, and the rate of evaporation was observed through a microscope and recorded on motion picture film.

The Air Stream and Measurement of Air Velocity. Metered dry air entered the bottom of a vertical 3¼-in. I.D., insulated tube, passed through a 200 W electric heater, and then through a 4 in. depth of 4 mm glass beads for distribution and an additional 4 in. depth of copper turnings for temperature stability. The tube was 40 in. long and terminated in a smoothly convergent nozzle of a shape suggested by Mache and Hebra, [22]. The nozzle opening was covered by a 140 mesh copper screen which made the velocity uniform over the opening and everywhere equal to the average volumetric velocity.
For velocities less than 300 cm s^{-1}, point velocity mapping with a hot wire anemometer of the type used by Ring, [19], showed that the screen evened the velocity distribution to the point where the volumetric rate through the flow meter gave an accurate measure of the central velocity. Velocity profiles taken 0.2 cm above the nozzle persisted to some distance. The anemometer did not detect velocity fluctuations over the screen until the wire was less than 0.1 cm from the opening. No indication of increased transfer due to turbulence created by the screen was noted in any of the tests.
Evaporation tests with air temperatures between 85 °C and 220 °C were made by suspending a drop on a fine filament over a hot, dry air stream and recording the history of evaporation on motion picture film. The hot air stream issued from a 25 mm I.D. glass tube clamped to a swinging arm, and was moved under the suspended drop at the moment an evaporation test was started. The tube was filled with glass beads and covered with a 140 mesh screen, so that a uniform distribution of velocity could be assumed.

Method of Drop Suspension. Drops were suspended from a glass capillary, sealed to the delivery tube of a microburette, which had a capacity of 0.01 mL in units of 10^{-5} mL. The capillaries were drawn so that the large end was the size of the ground glass tip of the microburette and the small end was 60 to 100 µm in diameter. Since a drop would climb up the side of a plain glass capillary, they were coated with No. 9987 Dri-film to ensure that the drop hung freely from the tube.
This type of suspension system seemed to duplicate most nearly the case of a free drop. Much more than half the evaporation occurred on the side facing the air stream, and in this system the side presented to the air stream showed no protuberances. In addition, it was reasonable to believe ,that nearly the same type of eddying as that for a free drop occurred on the rear side, in contrast to what might be obtained if, for example, the drops were supported on horizontal wires or filaments. The suspended drop rotated at a linear velocity which appeared to be less than 1 % of the air velocity, and the rotation did not seem to be affected by the presence of the capillary. The effect of rotation was negligible in these experiments as it probably is in the evaporation of free drops falling at low Reynolds number. Figure 4.1 shows the burette in place with the capillary positioned vertically over the center of the nozzle opening. The bottom of the drop cleared the screen about 0.3 cm. Evaporation rates for constant diameter drops were determined by measuring the rate of feed through the burette necessary to maintain a constant diameter.

Measurement of Drop Diameter. Figure 4.1 and Figure 5.1 show pictures of the illumination and projection system used to observe the evaporating drop and measure its diameter. The drop image was projected and measured on the ground glass screen of a microscope camera. Figure 4.2 is a photograph of a drop as it appeared on the camera screen. Another microscope with long focal length objective and high-power eyepiece was used to observe the drop in reflected light and to aid in centering the thermoelement inside the drop. With room-temperature air, the diameter of a drop was easily kept within a tolerance of ±0.03 cm on the screen.
In tests with hot air and changing drop diameter, motion pictures were taken at a magnification of approximately 7 times on the film, and at a rate of 24 frames s^{-1}. Drop diameters were measured frame by frame on a microfilm viewer. In this case diameter and time measurements were a measure of the evaporation rate.

Measurement of Air Temperature and Drop Temperature. Air temperatures and drop temperatures were measured with calibrated thermoelements of 3 mil, 2 mil, 1 mil, and 1/2 mil manganin-constantan wire. The thermocouples were held between needles mounted in a wood block which was carried by a traversing mechanism that made it possible to move the junction in a horizontal plane above the nozzle (see Figure 4.1). Four couples were usually in operation at one time, 2 mil, 1 mil, and 1/2 mil wires being employed in series for extrapolation to a true temperature. It is

believed that temperature readings to the nearest 0.1 °C were obtained. During any one run (from 5 min to 20 min) the temperature of the air stream, measured by the fine thermoelements, never varied more than 0.2 °C and in most cases less than 0.1 °C. The air temperature was taken as the average temperature for the complete test run.
The temperature of the drop was measured by embedding a thermoelement junction inside the drop (see Figure 4.2). The junction had to be perfectly clean to accomplish this feat.
The thermocouple and its leads, the capillary, and the addition of sensible heat in the feed liquid, complicated the heat balance. An attempt was made to determine the magnitude of these various factors by taking temperature measurements under special conditions, for example, while feeding, while not feeding, with the capillary in place, and with the drop hanging from the thermoelement junctions. During evaporation tests, the thermoelement was removed so as not to disturb the flow pattern and provide an additional path for heat conduction. Consequently, the drop temperature for a test run was determined before the test by taking drop temperatures with 2 mil, 1 mil, and ½ mil thermoelements centered in a constant diameter drop being fed and evaporated under similar conditions as the test run.
For tests at 85 °C to 220 °C, the air temperature was measured with a high velocity copper-constantan thermocouple at the center line, 0.3 cm above the opening of the swinging air jet, and the drop temperature was approximated in separate tests by rapidly taking temperatures of drops suspended on thermoelements after the hot air stream was swung under the drop.
In every case measured drop temperatures were, for practical purposes, the same as wet bulb temperatures estimated from a standard psychrometric chart. The error in ΔT's approximated from a psychrometric chart was never more than 4 % for forced convection.

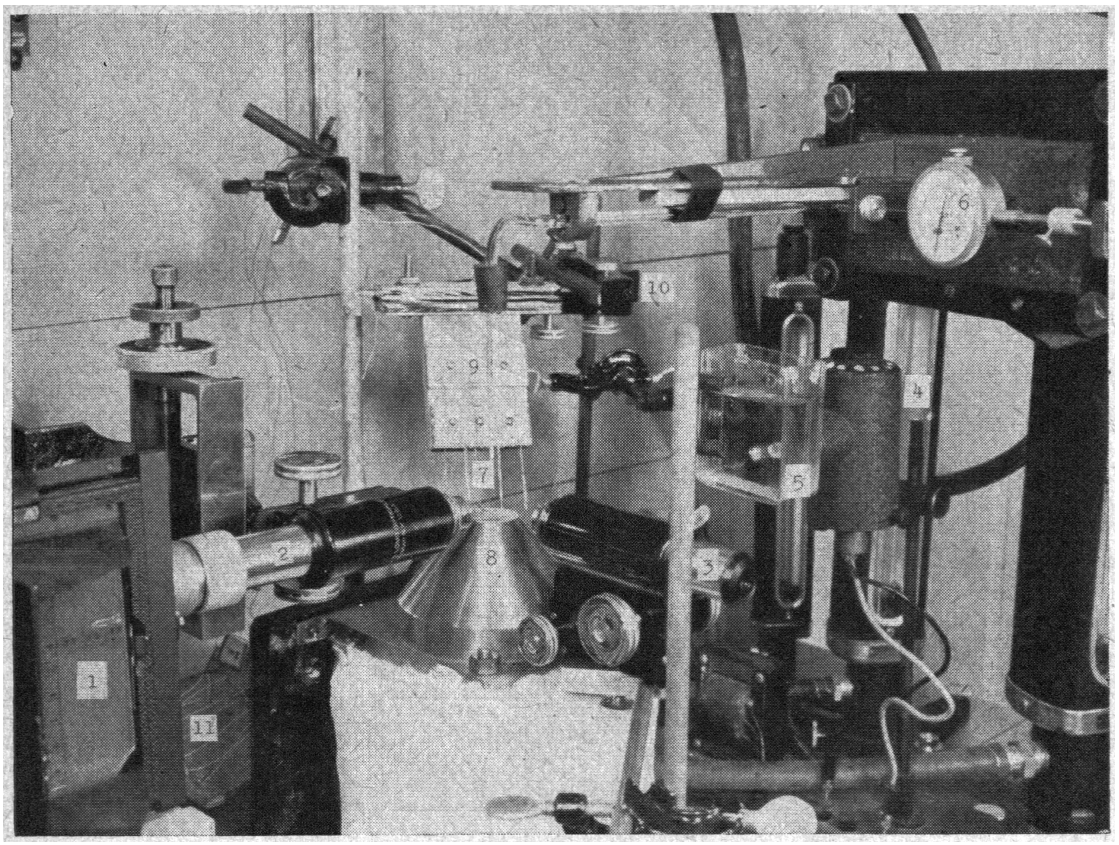

Figure 4.1.: Photograph of experimental equipment

1. Micam camera
2. Projection microscope
3. Viewing microscope
4. Projection light
5. Filter
6. Microburette
7. Suspension capillary
8. Nozzle
9. Thermoelement carrier
10. Traversing mechanism
11. Cold junction

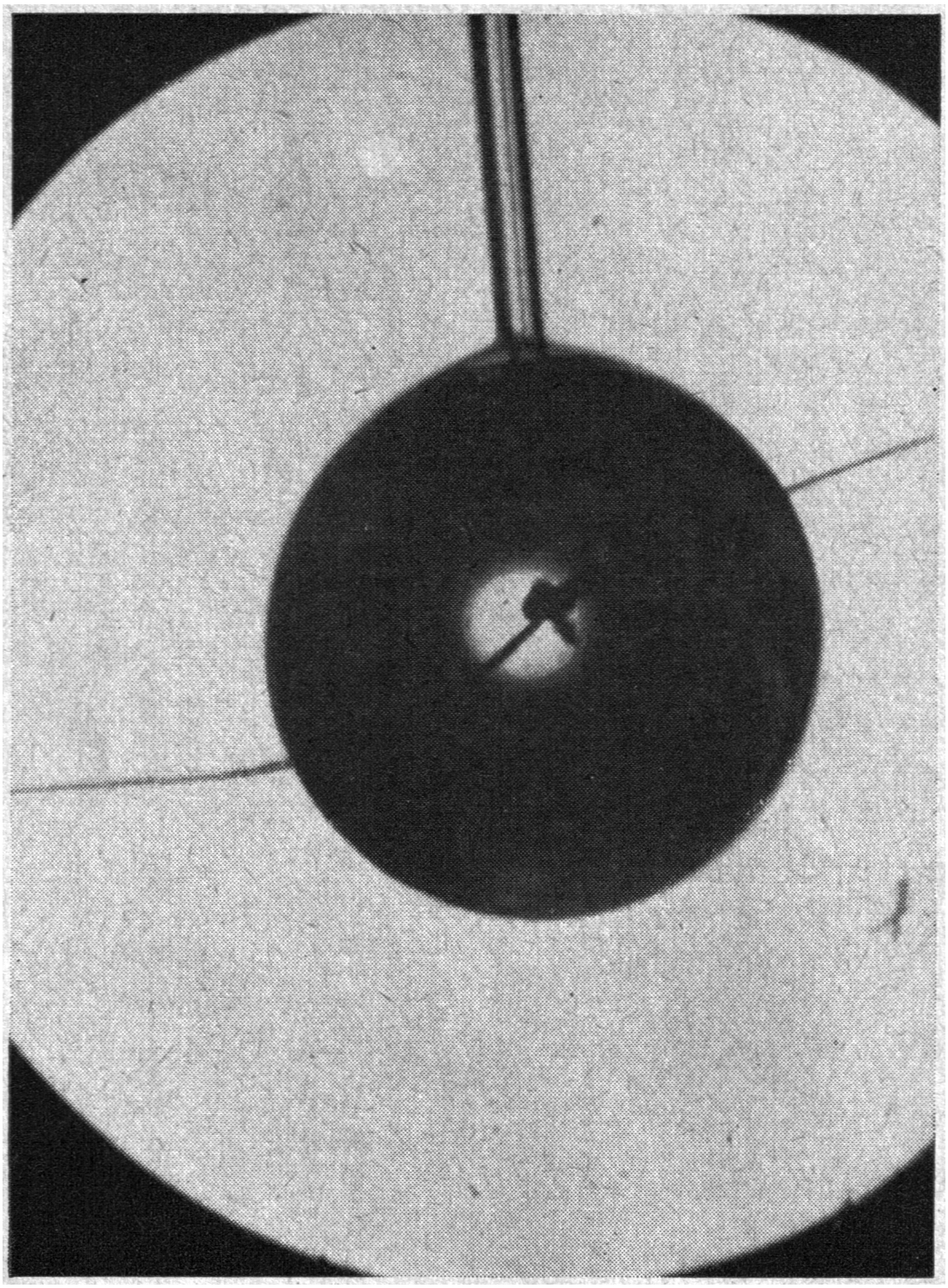

Figure 4.2.: Photomicrograph of an evaporating water drop, suspended from a feed capillary, with a ½ mil manganin-constantan thermoelement junction at its center. $D_p = 0.0945\,\text{cm}$; capillary diam. about 80 µm

5. Measurement of Evaporation from Drops in Still Air

Figure 5.1 shows a special dryer for the study of evaporation rates in still air. The bottom and upper portions of the drying unit with the exception of observation windows and probe holes were filled with silica gel, and the entrance holes for the thermoelement apparatus and burette tip were sealed with plasticine.
The drop evaporated with changing diameter as it hung on a thermoelement or with constant diameter as it hung on a capillary. The temperature difference, ΔT, was determined by an opposed-type thermoelement with junctions on a horizontal line one centimeter apart; the drop was suspended on one of the junctions.

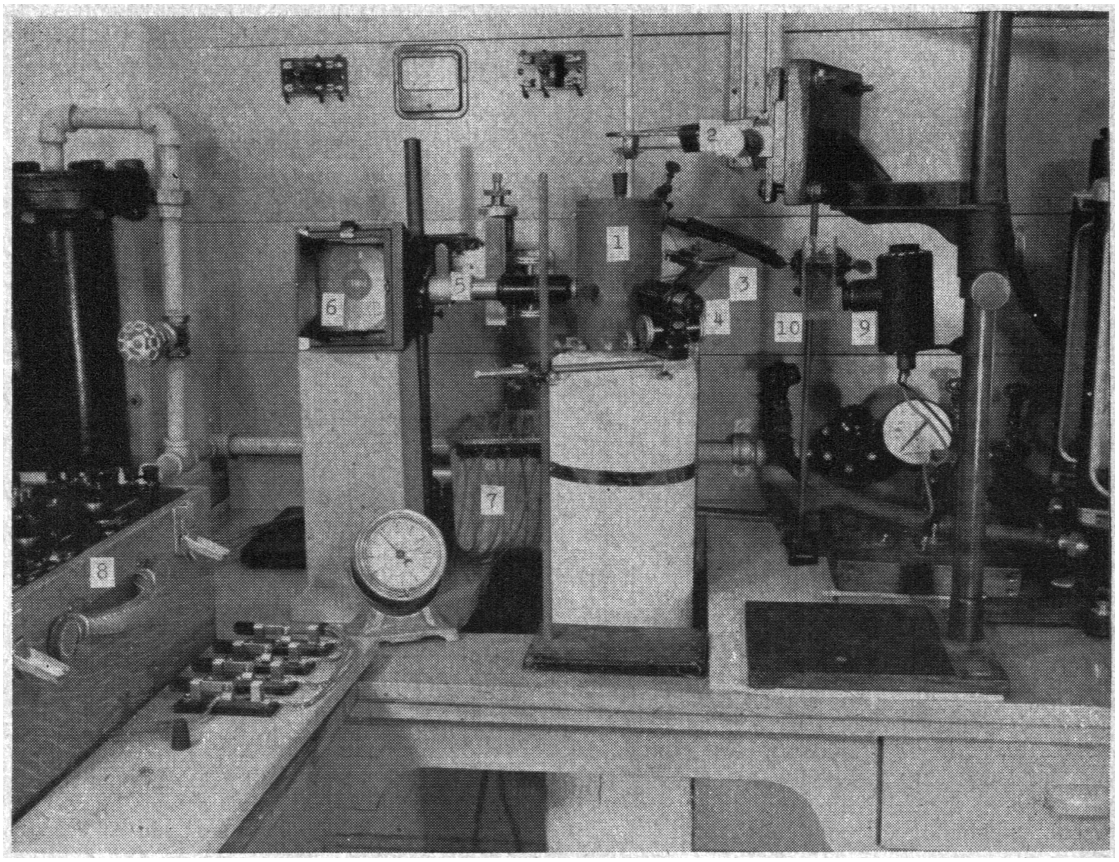

Figure 5.1.: Equipment for evaporation of drops in still air

1. Special dryer **2**. Microburette **3**. Thermoelement carrier **4**. Observation microscope **5**. Projection microscope **6**. Micam camera screen **7**. Cold junction **8**. Potentiometer **9**. Projection light **10**. Filter

6. Transport Properties of Air and Water Vapor

A critical review of the transport properties of air and water vapor was made to ensure reliable correlations of experimental data. The values used in calculations are given in graphical form by Figure 6.1, and the correlations presented later are dependent on these values.

Specific heats at constant pressure were taken from statistical mechanical calculations, [7], [8]. Viscosity values were obtained by calculations based on the LENNARD-JONES intermolecular potential, [3], [12], [13], [14], and are in close agreement with careful experimental measurements, [2], [15], [32]. Values of thermal conductivity are from the experimental data of TAYLOR and JOHNSON, [30], the values for temperatures above 380 ° K being obtained by extrapolation.

Recommended values of the diffusion coefficient of water vapor in air were calculated as a first approximation by R. B. BIRD, [12], [13], [14], from experimental measurements of the dipole moment and second Virial coefficient of steam and the polarizability of air. The calculated values agree excellently with the original data of WINKELMANN, [34], [35], [36], both in magnitude and temperature dependency but are approximately 10 % lower than that indicated by the S.T.P. value given by the *International Critical Tables*. A wide scattering of experimental values of diffusivity for air-water vapor mixtures are available, the latest work being that of SCHIRMER, [28]. However, every experimental method has involved a liquid-gas interface and a diffusion path of indefinite length. Because of such experimental difficulties (all the expected errors tend to give high values for $\mathscr{D}_v$), because of the experimental value of Nu' at $\mathrm{Re} = 0$ obtained in this study, and because of the greater consistency in calculated and experimental wet-bulb temperatures in this and related mass transfer operations, the theoretical values of $\mathscr{D}_v$ listed here are considered to be the most accurate. The only other phenomenon which could explain the observed facts and cause a high apparent $\mathscr{D}_v$ would be the modification of the widely accepted assumption that the partial pressure of vapor at a liquid surface of temperature T_i is the equilibrium vapor pressure at temperature T_i. This implies an accommodation coefficient of 1.0, which may or may not be true for water surfaces, [10].

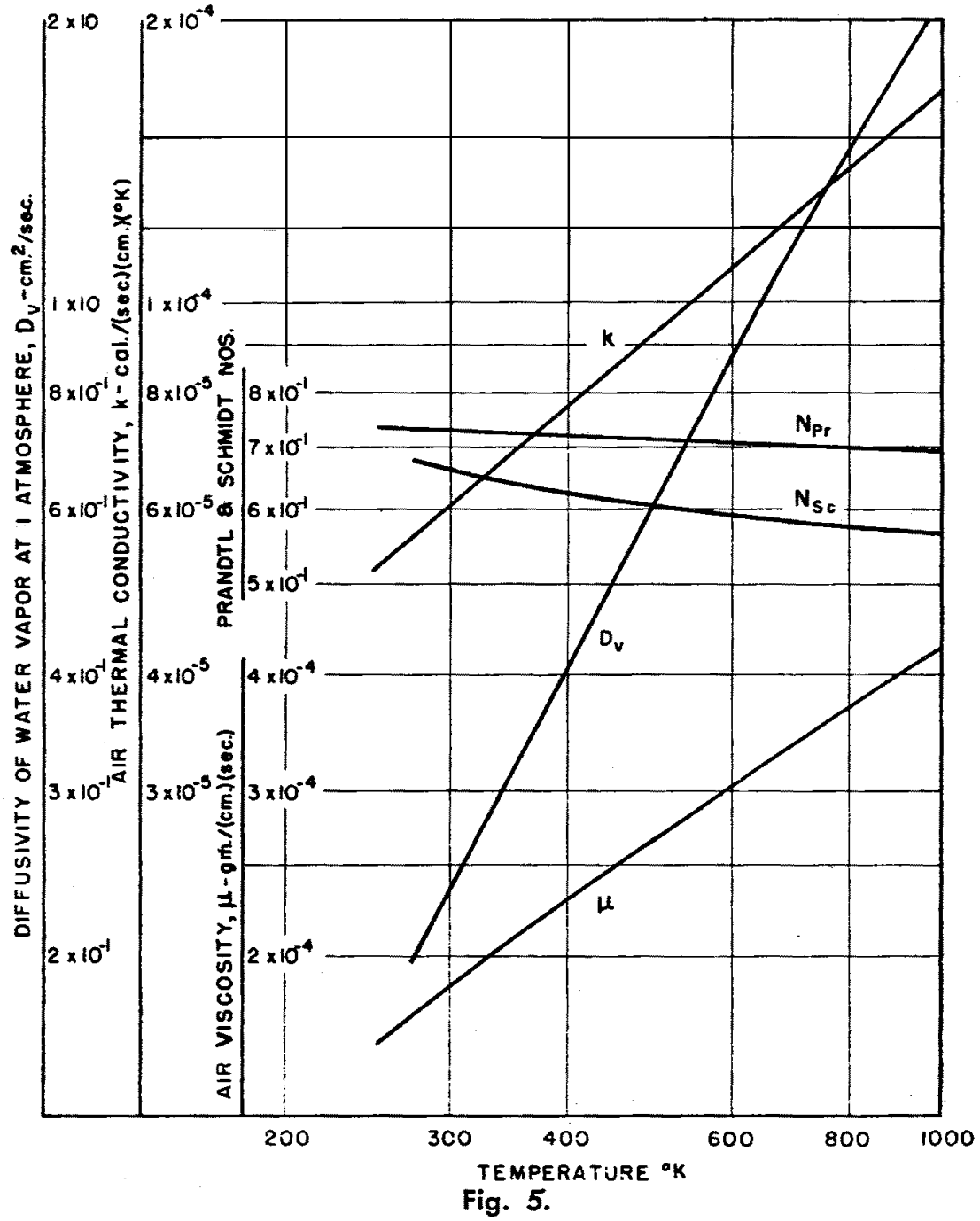

Figure 6.1.: Transport properties of air and water vapor-air mixtures as a function of Temperature

7. Calculation Procedures

To determine the experimental value of Nu Or Nu′ a major assumption made was that the surface temperature of the drop, T_i, was everywhere the measured value, and that the partial pressure of water vapor at the surface p_{Ai} was everywhere equal to the saturation partial pressure of water vapor at T_i. Since the thermal conductivity of water at 20 °C is 0.5987 W m^{-1} K^{-1}[1] or 25 times as great as that of air, the temperature of the drop was assumed uniform throughout and equal to the experimentally measured temperature. Actual measurements showed that the position of the thermoelement junction within the drop had no apparent effect on the indicated temperature.
The Nusselt group for mass transfer was determined by inserting the experimentally determined values and transport properties in the following equation:

$$\mathrm{Nu}' = \frac{r_{Aai} D_p \bar{M}_m p_f}{\Delta p_A \mathscr{D}_v \rho} \tag{7.1}$$

Since water vapor at most represented but 1 % of the gas mixture, the physical properties of the transfer path were taken as those of dry air at the arithmetic average temperature. No correction was made for the cross-sectional area of the capillary since it represented less than 0.2 % of the drop surface.
The Nusselt number for heat transfer was more difficult to obtain since sensible heat added in the feed, transferred by conduction along the capillary, and brought in by radiation had to be considered. Since the heat transferred by all methods must equal the latent heat of evaporation, a heat balance gives

$$\begin{aligned} q_{ai} = \lambda_i r_{Aai} = {} & h_c \Delta T \quad \text{(convection and conduction)} \\ & + r_{Aai} C_l \Delta T \quad \text{(sensible heat)} \\ & + \sigma\epsilon \cdot \left(T_o^4 - T_i^4\right) \quad \text{(radiation)} \\ & + r_{Aai} \lambda_i \cdot \left[\frac{\Delta(\Delta p_A)}{\Delta p_A}\right]_c \quad \text{(conduction along capillary)}\,. \end{aligned} \tag{7.2}$$

Equation 7.2 in terms of the Nusselt number becomes

$$\mathrm{Nu} = \frac{h_c D_p}{\kappa} = \frac{r_{Aai} \lambda_i D_p}{\Delta T \kappa} \cdot \left\{1 - \frac{\Delta T C}{\lambda_i} - \frac{4\sigma\epsilon T_o^3 \Delta T}{\lambda_i r_{Aai}} - \left[\frac{\Delta(\Delta p_A)}{\Delta p_A}\right]_c\right\} \tag{7.3}$$

[1] The original value is 1.43×10^{-3} cal./(sec.) (cm.)(°C)

where

$$\left[\frac{\Delta(\Delta p_A)}{\Delta p_A}\right]_c$$

is the percentage change in Δp_A caused by the presence of the capillary. This fractional change in partial pressure difference was determined by drop temperature measurements with and without the capillary in place. Equation 7.3 shows the true value of Nu as an apparent Nu corrected by a series of terms. For a typical test (No. 80) the values of the correction terms were as follows:

$$\begin{aligned}\mathrm{Nu} =& 5.83 \cdot (1 - 0.028 - 0.006 - 0.011)\\ =& 5.57\,.\end{aligned}$$

Since the corrections for radiation and capillary effects were small, and since the correction for sensible heat was excessive (about half of it was actually realized), only the sensible heat correction was made for the points on the correlation curve, the errors in this procedure tending to cancel one another.
Although evaporation and heat-transfer rates in still air were obtained at constant diameter, it was considered more accurate to support the drop on a fine thermoelement and determine evaporation rates from the change in drop diameter with time. From such measurements the Nusselt groups can be determined from the relations

$$\mathrm{Nu} = -\frac{1}{4} \cdot \frac{\lambda_i \rho_l}{\Delta T \kappa} \cdot \frac{\mathrm{d}D_p^2}{\mathrm{d}\tau} \tag{7.4}$$

$$\mathrm{Nu} = -\frac{1}{4} \cdot \frac{\rho_l \bar{M}_m p_f}{\Delta p_A \mathscr{D}_v \rho_M} \cdot \frac{\mathrm{d}D_p^2}{\mathrm{d}\tau} \tag{7.5}$$

Equation 7.4 and Equation 7.5 can be used also in the analysis of diameter vs. time data for drops evaporating at finite air velocities. In such an application the derivative of D_p^2 with respect to time varies with the instantaneous drop size.

8. Experimental Results for Pure Liquid Drops

Water Drops. Table 8.1 and Figure 8.1 present significant experimental results for evaporation from water drops. The points for heat transfer extrapolate close to the theoretical minimum value. Experimental values obtained for Nu at $\mathrm{Re} = 0$ were slightly greater than 2.0, and the small difference is attributed to free convection. Although the data for heat transfer involved an inherently inaccurate correction for sensible heat, this correction was small; and because values of thermal conductivity are more reliable than values of diffusivity, the heat-transfer points are believed to be more accurate than the mass-transfer points. Data for mass transfer show a steeper slope and a lower intercept, but the disagreement is always less than 10 % at a given Re and is usually much less than 5 %. Factors which may have contributed to errors in the data and anomalies in the heat- and mass-transfer analogy were:

1. inaccurate values of diffusivity.
2. p_{Ai} may not have been the saturation vapor pressure.
3. the partial pressure of water vapor in the air may not have been zero at low air rates where the air stream velocity and the velocity of free convection were of the same order of magnitude and water vapor from the room air diffused into the jet.
4. free convection may have been significant at low values of the air velocity.

						$\underbrace{\frac{hD_p}{\kappa} = \mathrm{Nu}}$		$\frac{\kappa g \bar{M}_m D_p p_f}{\mathscr{D}_v \rho}$	$\frac{D_p v_0 \rho}{\mu}$
Evap. rate, $\mathrm{mL\,s^{-1}}\cdot 10^5$	Drop. diam., cm	Air veloc., $\mathrm{cm\,s^{-1}}$	Air Temp., °C	Drop Temp., °C	Atmos. Press., mm Hg	Apparent	Corrected	Nu′	Re
0.392	0.0954	246.0	19.9	5.4	743	9.07	8.85	8.67	159.1
0.445	0.0954	210.0	24.6	7.6	740	8.68	8.44	8.35	132.4
0.416	0.0954	172.3	24.9	7.7	740	8.05	7.80	7.70	108.4
0.388	0.0954	153.2	25.3	7.9	740	7.40	7.19	7.08	96.2
0.354	0.0954	119.7	25.4	8.0	740	6.74	6.54	6.41	75.1
0.320	0.0954	95.2	24.3	7.6	738	6.34	6.16	5.98	59.9
0.294	0.0954	76.2	24.4	7.6	738	5.83	5.66	5.47	47.9
0.277	0.0954	57.1	24.5	7.7	738	5.49	5.33	5.12	35.9
0.274	0.0954	57.1	24.5	7.7	738	5.44	5.29	5.07	35.9
0.227	0.0954	28.5	24.6	8.0	738	4.54	4.41	4.11	17.91
0.1890	0.0954	15.13	24.7	8.0	738	3.76	3.66	3.42	9.49
0.1839	0.0954	11.78	24.8	8.1	738	3.63	3.53	3.32	7.39
0.1674	0.0954	8.41	24.9	8.9	738	3.35	3.26	2.96	5.27
0.1479	0.0954	3.37	25.0	8.5	738	2.97	2.89	2.58	2.11
0.459	0.0954	286.0	23.2	6.9	746	9.43	9.17	9.07	183.2
0.461	0.0954	267.0	23.6	6.1	746	9.34	9.09	9.01	170.0
0.433	0.0954	228.0	23.7	7.3	746	8.76	8.51	8.36	145.7
0.492	0.0954	306.0	24.0	7.3	746	9.84	9.56	9.48	195.0
Still Air		0.0	24.9	9.1	741	2.23	—	1.79	0

Note: Drop temperatures measured with 0.5 mil thermocouples.

Table 8.1.: Experimental results for Evaporation of water drops in dry air

						$\underbrace{\frac{hD_p}{\kappa} = \mathrm{Nu}}$		$\frac{\kappa g \bar{M}_m D_p p_f}{\mathscr{D}_v \rho}$	$\frac{D_p v_0 \rho}{\mu}$
Evap. rate, $\mathrm{mL\,s^{-1}}\cdot 10^5$	Drop. diam., cm	Air veloc., $\mathrm{cm\,s^{-1}}$	Air Temp., °C	Drop Temp., °C	Atmos. Press., mm Hg	Apparent	Corrected	Nu′	Re
1.47	0.085	230	90	–	740	7.9	7.3	7.0	101
0.90	0.085	110	77.5	–	740	5.9	5.3	5.3	50
0.91	0.085	110	78.7	–	740	5.8	5.3	5.3	50
0.91	0.085	110	78.7	–	740	5.9	5.4	5.3	50
1.56	0.095	183	84.0	27.8	746	8.1	7.3	7.2	93
1.16	0.095	114	82.5	27.6	744	6.2	5.6	5.4	58
1.17	0.095	114	83.0	27.8	744	6.2	5.6	5.4	58
0.73	0.095	55	66.4	24.1	744	4.9	4.5	4.3	29
0.62	0.095	17.6	71.4	24.8	744	8.7	3.4	3.5	9

Note: Where the drop temperature was not determined experimentally, the temperature of adiabatic saturation was assumed.

Table 8.2.: Data for evaporation of water drops at air temperatures from 70 to 90 °C

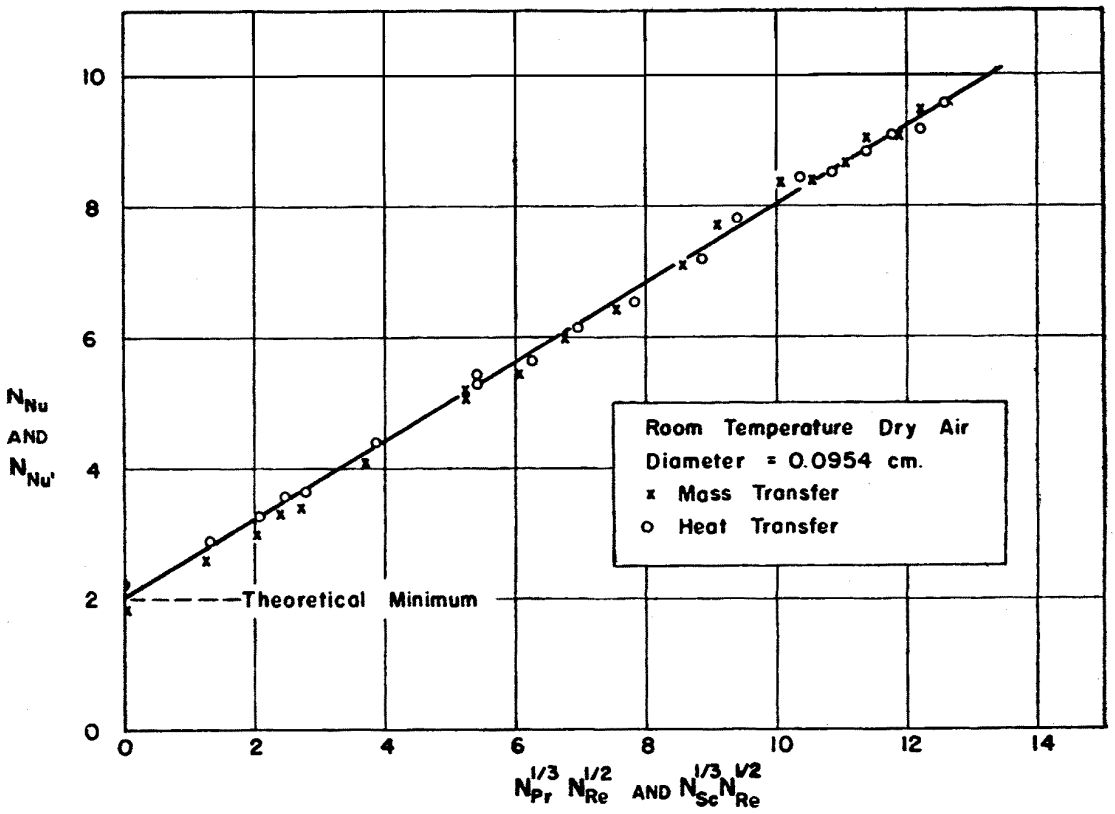

Figure 8.1.: Heat and mass-transfer correlation for evaporating water drops

Figure 8.2 shows results for water drops evaporating into room temperature air where drop temperatures were not taken but estimated to be the adiabatic saturation temperature of the air. Figure 8.2 includes the data of FRÖSSLING, [10] for water drops with diameters in a range from 0.064 to 0.18 cm. Figure 8.2 suggests three conclusions: (1) there is no diameter effect not accounted for by Re; (2) the assumption of a drop temperature corresponding to the temperature of adiabatic saturation in the case of water vapor-air mixtures is justified; (3) experimental results of FRÖSSLING and this investigation are the same, and differences occur only in analysis and interpretation of data.

Figure 8.3 shows a linear plot of D_p^2 vs. τ for an example evaporation test in still air. Since $\frac{\mathrm{d}D_p^2}{\mathrm{d}\tau}$ is constant, Nu and Nu′ are constant for all D_p. Substitution of experimental values for Figure 8.3 into Equation 7.4 and Equation 7.5 gives

$$\mathrm{Nu} = 2.23$$

and

$$\mathrm{Nu}' = 1.79\,.$$

If it is assumed that $\mathrm{Nu}' = 2.0$ at $\mathrm{Re} = 0$, then the data for still air can be used to

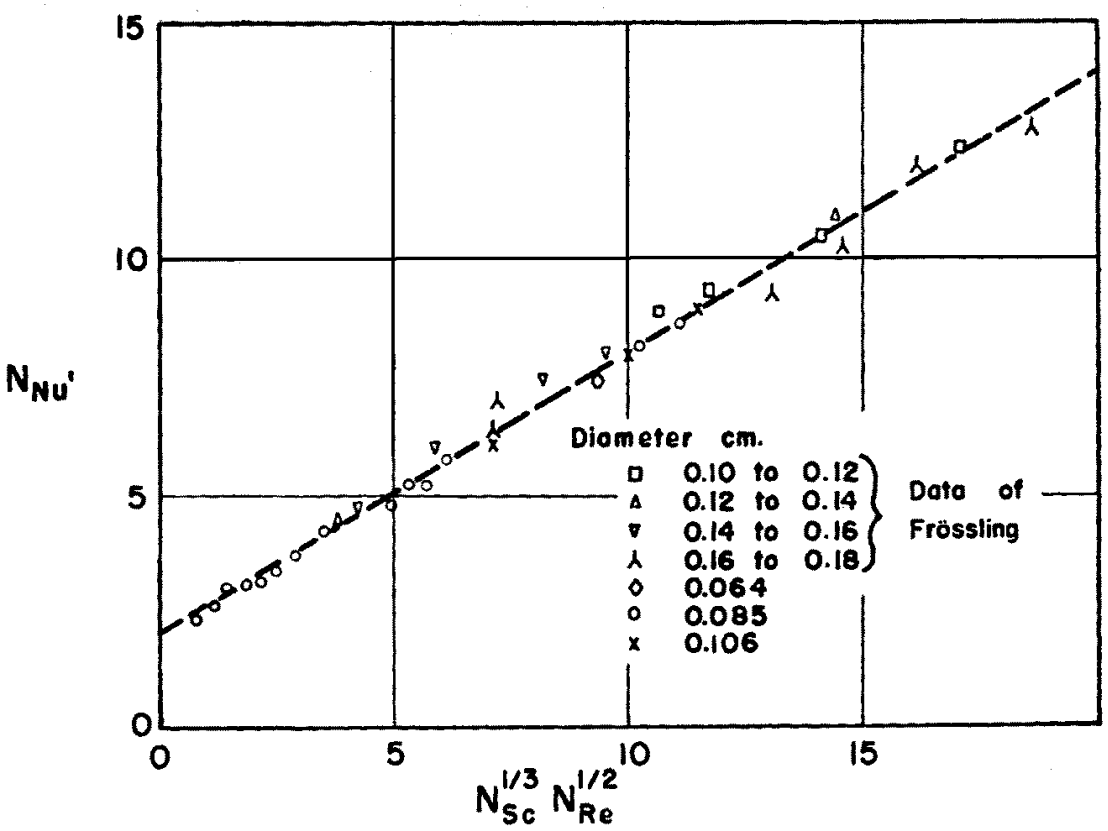

Figure 8.2.: Mass-transfer of evaporating water drops
Drop temperature assumed equal to the wet bulb

obtain $\mathscr{D}_v = 0.204\,\mathrm{cm^2\,s^{-1}}$ at an average temperature of 290 °K and a pressure of 741 mm Hg, a low value compared with other methods of determination.
Table 8.2 and Table 8.3 and Figure 8.4 show results for water drops evaporating at constant diameter into air at 66 °C to 90 °C. and for suspended water drops evaporating with changing diameter into air at 85 °C to 221 °C. Values of Nu for drops evaporating in hot air were calculated making the following assumptions: (1) T_{avg} was taken as the temperature at which the thermal, conductivity in the transfer path should be taken; (2) the drop was considered to be spherical and with all of its surface available for transfer; (3) in estimating thermal conductivity the transfer path was considered to contain only air; and (4) the main air stream was considered to be of uniform temperature and velocity distribution.

For suspended drops evaporating in air at 85 °C to 221 °C, Nu was obtained by applying Equation 7.4 and Equation 7.5 to an analysis of the motion picture record. Values of Nu′ are not reported for drop temperatures above 40 °C, because a small error in T_i causes such a large error in p_{Ai} that the results have no significance. Although Nu for T_o of the order of 200 °C, calculated as outlined, tended to fall below the curve obtained for room temperature air, the difference was of the order

$-\frac{dD_p^2}{d\tau}$ $cm^2\,s^{-1}$	D_p corresp. to $-\frac{dD_p^2}{d\tau}$ cm	Air veloc., $cm\,s^{-1}$	Air Temp., °C	Drop Temp., °C	$\frac{hD_p}{\kappa}$ Nu	$Re^{\frac{1}{2}}\,Pr^{\frac{1}{3}}$
$2.63e^{-4}$	0.085	184.0	115	35.6	7.0	7.7
2.07	0.071	184.0	115	35.6	5.5	7.0
0.89	0.056	18.8	85	29.4	3.6	2.1
0.71	0.049	18.8	85	29.4	2.9	2.0
5.3	0.096	184.0	221	52	5.7	7.2
4.2	0.058	184.0	221	52	4.5	5.6
3.3	0.088	77.0	193	49	4.2	4.6
3.2	0.060	77.0	193	49	4.0	3.8
1.56	0.101	21.0	125	38.3	3.7	2.8

Table 8.3.: Evaporation of water drops in dry air at elevated temperatures. Data from motion picture record

of magnitude of the error involved in obtaining the data, and the correlations of Figure 8.1 were not impaired.
Equations for the correlation in Figure 8.1 were obtained as follows:

$$\mathrm{Nu} = 2.0 + 0.60 \cdot \mathrm{Pr}^{\frac{1}{3}}\,\mathrm{Re}^{\frac{1}{2}} \tag{8.1}$$

$$\mathrm{Nu} = 2.0 + 0.60 \cdot \mathrm{Sc}^{\frac{1}{3}}\,\mathrm{Re}^{\frac{1}{2}} \tag{8.2}$$

Benzene Drops. Table 8.4 and Figure 8.6 show results for the evaporation of supercooled benzene drops in room temperature dry air. The drops evaporated. while suspended from a capillary and their temperatures were measured with a 1/2-mil manganin-constantan thermoelement. Since the drops assumed a tear-drop shape with the diameter along the axis of the capillary about 8 % greater than across the axis, D_p, was taken as the arithmetic average of the two diameters. The diffusivity was calculated by the methods of Hirschfelder, Bird and Spotz, [12], [13], [14].

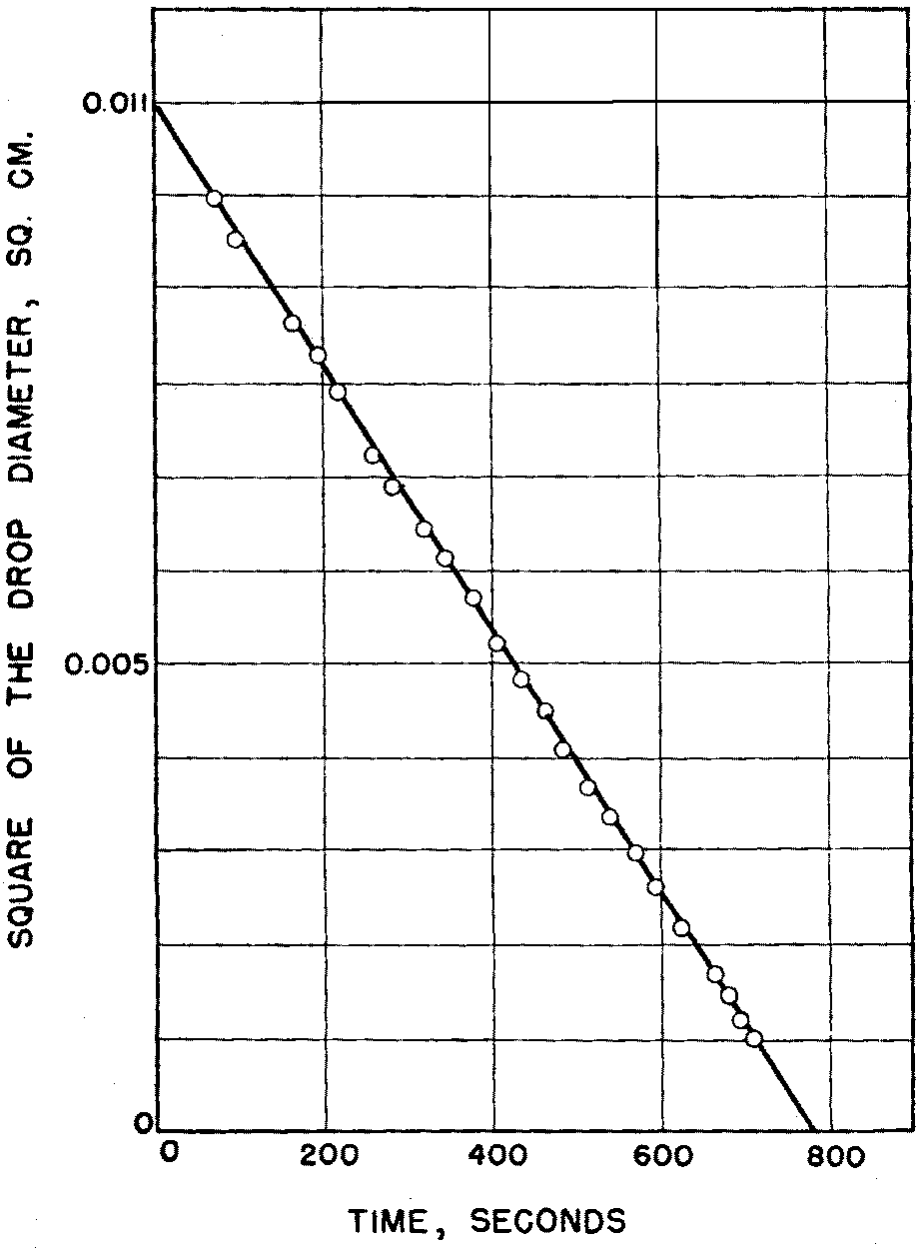

Figure 8.3.: Evaporation of water drop in still dry air

$T_o = 24.9\,^{\circ}\mathrm{C}$
$T_i = 9.11\,^{\circ}\mathrm{C}$
$\pi = 741\,\mathrm{mm\,Hg}$ (987.9 mbar)

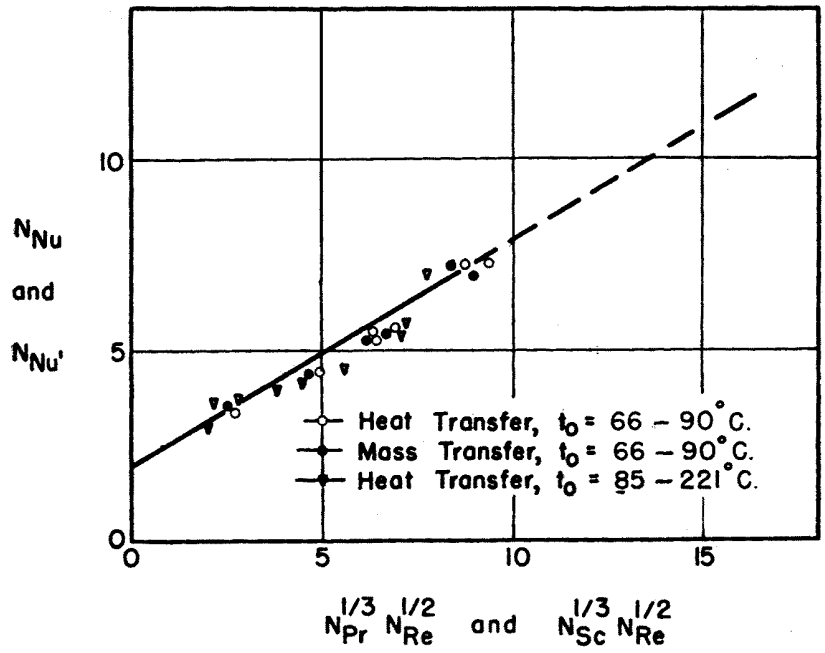

Figure 8.4.: Transfer rates in hot dry air

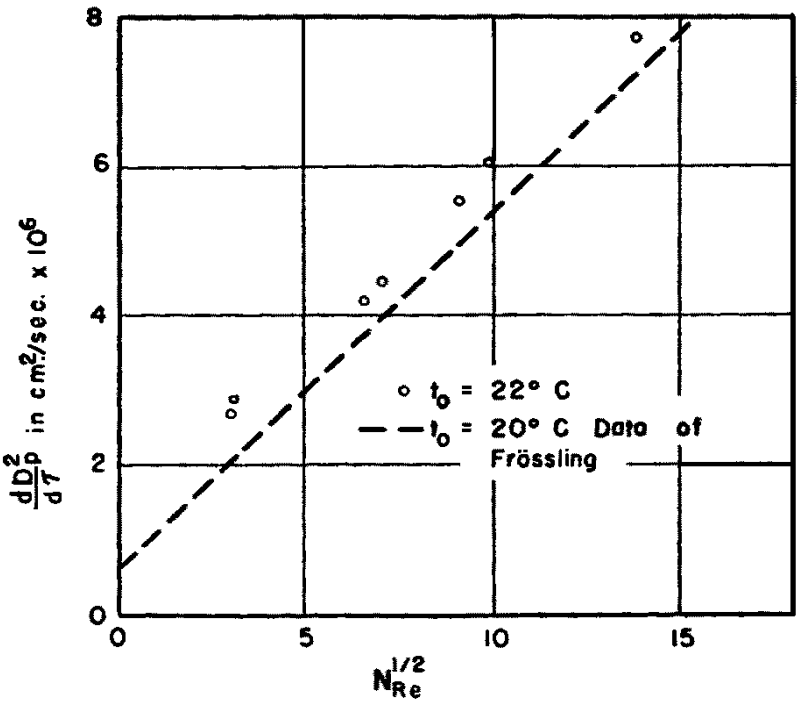

Figure 8.5.: Evaporation rates of aniline drops

Evap. rate, $mL\,s^{-1}$ $\cdot 10^5$	Drop diam., cm	Air veloc., $cm\,s^{-1}$	Air Temp., °C	Drop Temp. °C	Atmos. Press. mm Hg	$\frac{hD_p}{\kappa} = \mathrm{Nu}$ Apparent	$\frac{\kappa g \bar{M}_m D_p p_f}{\mathscr{D}_v \rho}$ Nu′	$\frac{D_p v_0 \rho}{\mu}$ Re
1.51	0.110	5.1	24.4	3.5	732	3.3	3.2	3.7
2.10	0.110	15.3	26.4	3.4	732	4.2	4.5	11.1
2.54	0.110	28.9	27.1	3.1	736	4.9	5.5	21.0
2.65	0.110	74.8	17.9	−1.8	739	6.3	7.8	57.0
2.96	0.110	112.4	17.5	−2.3	739	7.1	9.0	86.0
3.42	0.110	150.0	17.7	−2.2	739	8.1	10.3	115.0
1.82	0.110	18.8	20.7	0.0	733	4.1	4.8	14.1
2.02	0.110	28.3	20.4	−0.4	733	4.5	5.4	21.0
2.80	0.110	75.5	19.9	−1.0	733	6.3	7.7	56.0
3.21	0.110	113.0	20.0	−1.1	733	7.1	8.9	84.0
3.60	0.110	151.6	20.2	−1.1	733	7.9	10.0	113.0
3.95	0.110	190.0	20.2	−1.0	733	8.7	10.9	142.0
4.60	0.110	288.0	20.4	−0.94	733	10.1	12.6	220.0

Table 8.4.: Data for evaporation of benzene drops

$T_o = 21.7\,°C$ $D_p = 0.0954\,cm$ Capillary diam. $= 63\,\mu m$		$T_o = 21.7\,°C$ $D_p = 0.110\,cm$ Capillary diam. $= 74\,\mu m$	
Drop temp., °C	Reynolds No.	Drop temp., °C	Reynolds No.
7.3	2.11	1.1	2.5
7.3	9.55	−0.05	11.3
7.2	18.05	−0.1	21.3
7.1	48.0	−0.3	57.0
6.95	96.0	−0.85	114.0
7.0	120.2	−1.0	142.0
6.95	182.2	−1.05	215.0

Table 8.5.: Drop temperature as a function of Reynolds number

Avg. Conc. % NH_4NO_3	Air Temp. °C	Wet Bulb Temp. °C	Drop Temp. °C	Calc. Rate, $mL\,s^{-1}$	Exp. Rate $mL\,s^{-1}$
26	28.2	9.4	12.0	$0.360e^{-5}$	$0.368e^{-5}$
46	29.4	9.5	12.0	0.364	0.367
50	28.5	9.5	12.0	0.366	0.365

Table 8.6.: Evaporation rates for drops containing NH_4NO_3

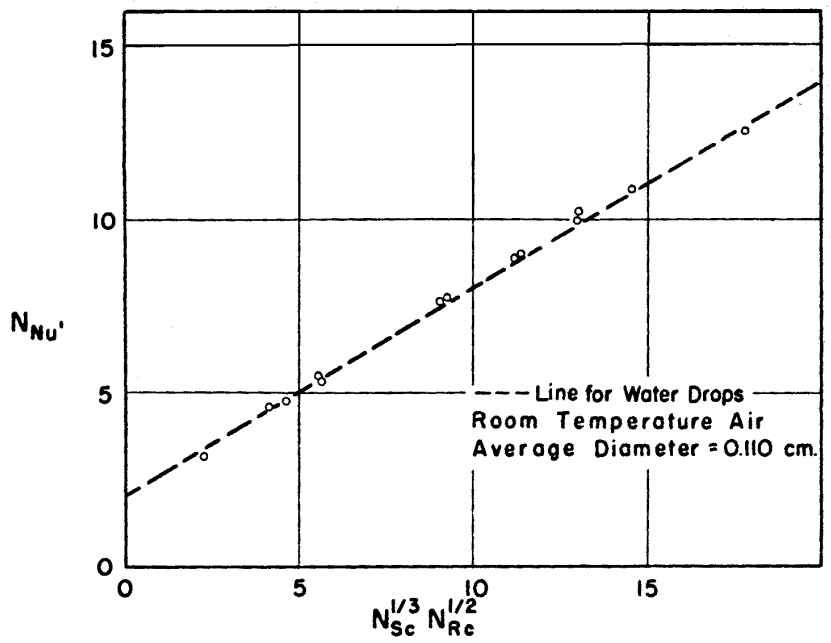

Figure 8.6.: Mass-transfer correlation of evaporating benzene drops

The agreement with the mass-transfer correlation given by Equation 8.2 is excellent. Since $\Delta T/\lambda_i$ for benzene represents about 20 % of the total heat flow to the drop, no attempt was made to obtain Nu. However, if approximately one half of the apparent sensible heat flow was realized, the values of Nu for the evaporation of benzene were in agreement with Equation 8.1. This indicates that the average temperature of the feed liquid entering the drop was about that of the air stream one and one-half drop diameters above the drop.

Aniline Drops. Evaporation rate data, for aniline drops suspended in a constant velocity air stream were taken to check the work of FRÖSSLING, [10], and to determine the accuracy of his technique for substances of low volatility. For comparison, values of $\frac{\mathrm{d}D_p^2}{\mathrm{d}\tau}$ vs. $\sqrt{\mathrm{Re}}$ are shown in Figure 8.5 along with the results of FRÖSSLING's work. An uncertainty in this correlation was the value of the vapor pressure of aniline, which was quite small. Using the single value of MACK, [23], in the low-temperature range and making corrections for comparison between data at 22 °C and 20 °C, the experimental results expressed as $\frac{\mathrm{d}D_p^2}{\mathrm{d}\tau}$ appear to be in reasonable agreement with those of FRÖSSLING. However, with the indicated Δp_A, values of Nu′ were nearly 10 % lower than the correlation obtained for water drops, and the slope of the line was 0.55 as FRÖSSLING suggested.

9. Discussion of Results on Evaporation from Pure Liquid Drops

9.1. Comparison with Other Data

In Figure 9.1 results of this investigation and the correlation of Equation 8.1 and Equation 8.2 were compared with experimental data from the literature. Data of Frössling, [10], and Maisel and Sherwood, [24] were corrected to the value of $\mathscr{D}_v$ for water vapor used in this study. Data of Kramers, [20], deviate from the correlation at low values of the Reynolds number because of free convection. Other data reviewed by Williams, [29], can also be shown to agree with this correlation.

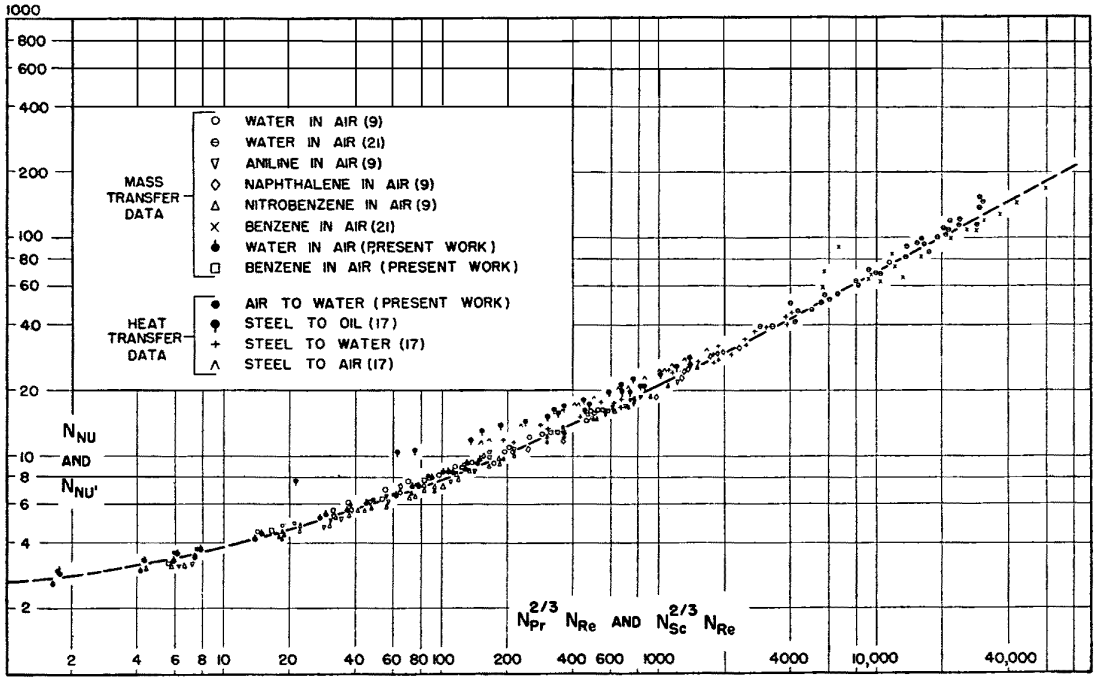

Figure 9.1.: Correlation of mass- and heat-transfer rates for single particles, – – – – – – – – – – Equation 8.1 and Equation 8.2

Figure 9.1 shows that the results of this investigation merged smoothly into the results of other investigations at higher Reynolds number, and that the empirical Equation 8.1 and Equation 8.2 are remarkably accurate even when extrapolated five times beyond the experimental range in which they were determined. The overall success of this correlation gives credence to the values of the exponents on Pr, Sc and Re as well as an implication that the calculated value of the diffusivity of water vapor in air may be more accurate than any reported in the literature.

9.2. Free Convection

Figure 9.2 presents evidence of free convection for the evaporation of water drops at constant diameter in still dry air. These experimental data for $\mathrm{Re} = 0$ agree with Equation 3.12 shown by the dashed line. However, the experimental technique was not sensitive to free convection because the inherent errors involved were of the same order of magnitude as the effect and difficult to isolate. In contradiction, Figure 8.5 for the evaporation of a drop in still air with changing diameter indicated no free convection since the plotted points were on a straight line and T_i remained constant. within 0.05 °C down to a droplet of minute size. To show the effectiveness of Equation 3.12 beyond the range of this investigation, experimental data of Meyer, [26], and Elenbaas, [9], were plotted in Figure 9.2. Little consideration has been given to the experimental errors caused by free, convection. In the work of Frössling, [10], and in this investigation, free convection tended to oppose the main velocity; in the work of Kramers, [20], it aided the main velocity; and in the work of Maisel and Sherwood, [24], it partially aided in increasing transfer rates.

9.3. Drop Temperatures

To determine experimentally the temperatures of drops. at various Reynolds numbers, the data of Table 8.5 were taken. In these tests a mil thermocouple was inserted in the drop during evaporation, and the temperature was measured when the drop had evaporated to the desired diameter and when no liquid was being fed through the capillary.
For no extraneous heat effects, the ratio of Equation 8.1 and Equation 8.2 indicates that $\frac{\Delta p_A}{\Delta T}$ should increase with increased Re where $\mathrm{Pr} > \mathrm{Sc}$. For water drops where Pr is slightly larger than Sc, the opposite seemed to be true although the trend was slight. For most practical purposes the temperature of a water drop can be taken constant for all Reynolds numbers. For benzene drops where Sc was relatively much larger than Pr, the expected result of decreased $\frac{\Delta p_A}{\Delta T}$ and decreased T_i was realized since extraneous heat effects were not large enough to influence the general trend of the results.

At high air temperatures, measurement of the drop temperature was more difficult. The experimental drop temperatures in Table 8.3 for air temperatures above 85 °C were averaged over temperature ranges of about 5 °C. Temperature lag was due to the fact that the drop started out at a temperature of roughly 10 °C and a high heat flux was required to bring it up to T_i. Experimental values of drop temperature for dry air at 220 °C appeared to be about 2 °C higher than the temperature of adiabatic saturation.
For practical purpose, the temperature of adiabatic saturation is a good approximation to the temperature of evaporating water drops. For liquids other than water only wet-bulb temperatures should be used to estimate the temperatures of the drop.

9.4. Extrapolation of Results to Higher Air Temperatures

At air temperatures of the range 300 °C to 500 °C, Equation 8.1 and Equation 8.2 must be used with care. From a practical standpoint Equation 8.1 for heat transfer is the preferred relationship for estimating evaporation rates at all temperatures since the thermal conductivity is better known than the vapor diffusivity. Its use, however, requires a value of, drop temperature. This temperature can usually be taken as the wet-bulb temperature, and in the case of water the adiabatic saturation temperature. If radiation is contributing to heat flux, its effect must be estimated to obtain accurate evaporation rates. The principal problem associated with high temperature is the proper averaging of the transport properties over a short transfer path. These properties may vary two- to fivefold in the boundary film. It is necessary, then, that a study of transfer phenomena at higher temperatures in dynamical systems. be preceded by a more accurate determination of the values of transport properties and by a study of the effect of large gradients. In addition, other phenomena, such as thermal diffusion and transport of sensible heat by the diffusing component, should be considered under these conditions.

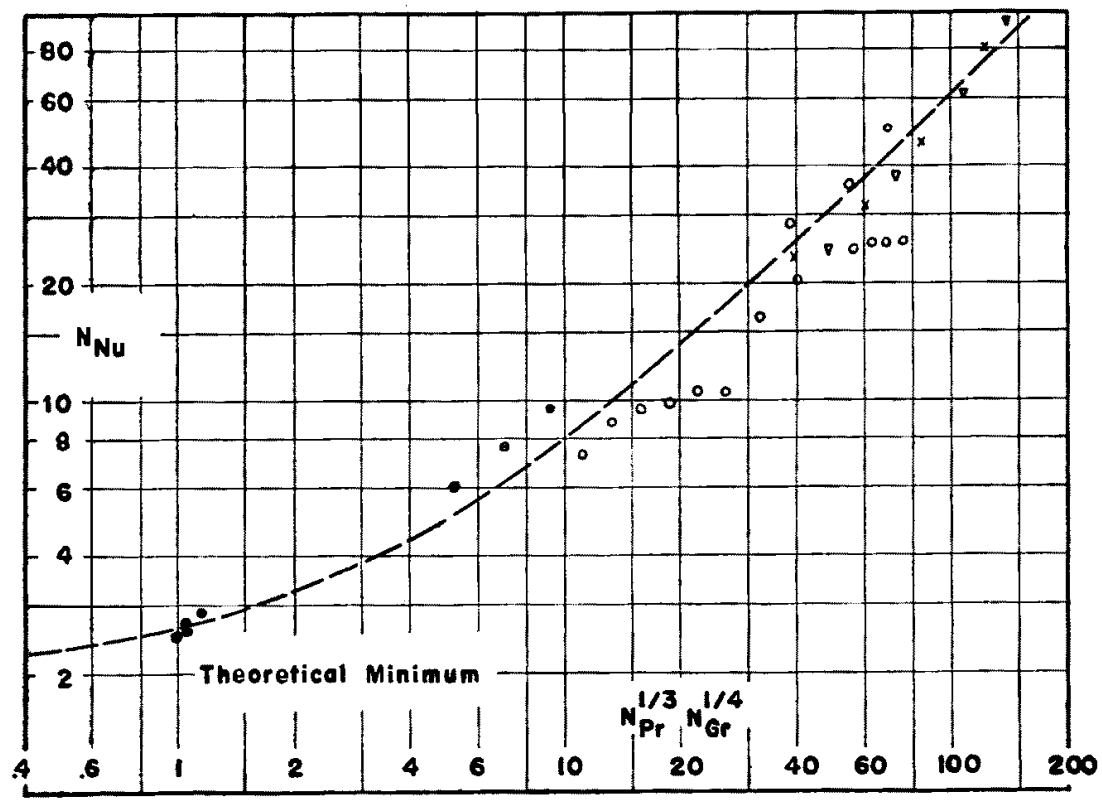

Figure 9.2.: Free convection for spheres

Air to evaporating water drop
Ice to water at 15 °C [26]
ice to water at 30 °C [26]
Ice to water at 45 °C [26]
Silver sphere cooling in air [9]
correlation Line:
$\mathrm{Nu} = 2.0 + 0.60 \cdot \mathrm{Pr}^{\frac{1}{3}}\,\mathrm{Gr}^{\frac{1}{2}}$

10. Evaporation from Drops Containing Solids in Solution and Suspension

10.1. Water Drops Containing Soluble Salts

A study was made of the assumption that water drops containing substances which lower the normal vapor pressure evaporate as though the drop surface was saturated regardless of the average concentration of the drop. Drawn up into the microburette were 5×10^{-5} mL of aqueous solutions of various concentrations of NH_4NO_3, and they were fed out as a drop of 0.106 cm in diameter, and the rate at which water had to be added to keep the drop at constant diameter was measured.
To estimate the temperature of the evaporating drop according to the above simplifying assumption, the adiabatic saturation line for the air conditions was drawn on a standard psychrometric chart. The intersection of this line with the line of partial pressure of water vapor over saturated aqueous solutions of NH_4NO_3, located p_{Ai} and T_i for the surface of the drop. Such a graphical solution for T_i is shown in Figure 10.1, where the partial pressure of water over saturated solutions of NH_4NO_3 is taken from Adams and Merz, [1]. For. other liquids, the slope of the line must be determined from the ratio of the heat- and mass-transfer coefficients and not from an adiabatic saturation line.

Table 6 shows experimental and calculated values of evaporation rates where the calculated rate is the rate for pure water drops, based on Equation 8.1, corrected for sensible heat and for the reduced vapor pressure of a saturated solution. Even with the added internal turbulence due to feeding make-up solvent and the low evaporation rates with room temperature air, the evaporation rate for all concentrations was nearly that for the saturated aqueous solution of NH_4NO_3 at 12 °C. Therefore, the assumption of saturation at the drop surface, regardless of the average drop concentration, appeared to be confirmed.
Similar tests with sodium chloride solutions did not give such clear-cut results since the saturation concentration of salt is low (about 26 %) and has a much smaller effect on the vapor pressure of the solvent.
In applications with air temperatures of the order of 250 °C, the ratio of ΔT's for saturated solutions and pure water approach unity and the effect of solid in solution would become negligible in the constant-rate period.

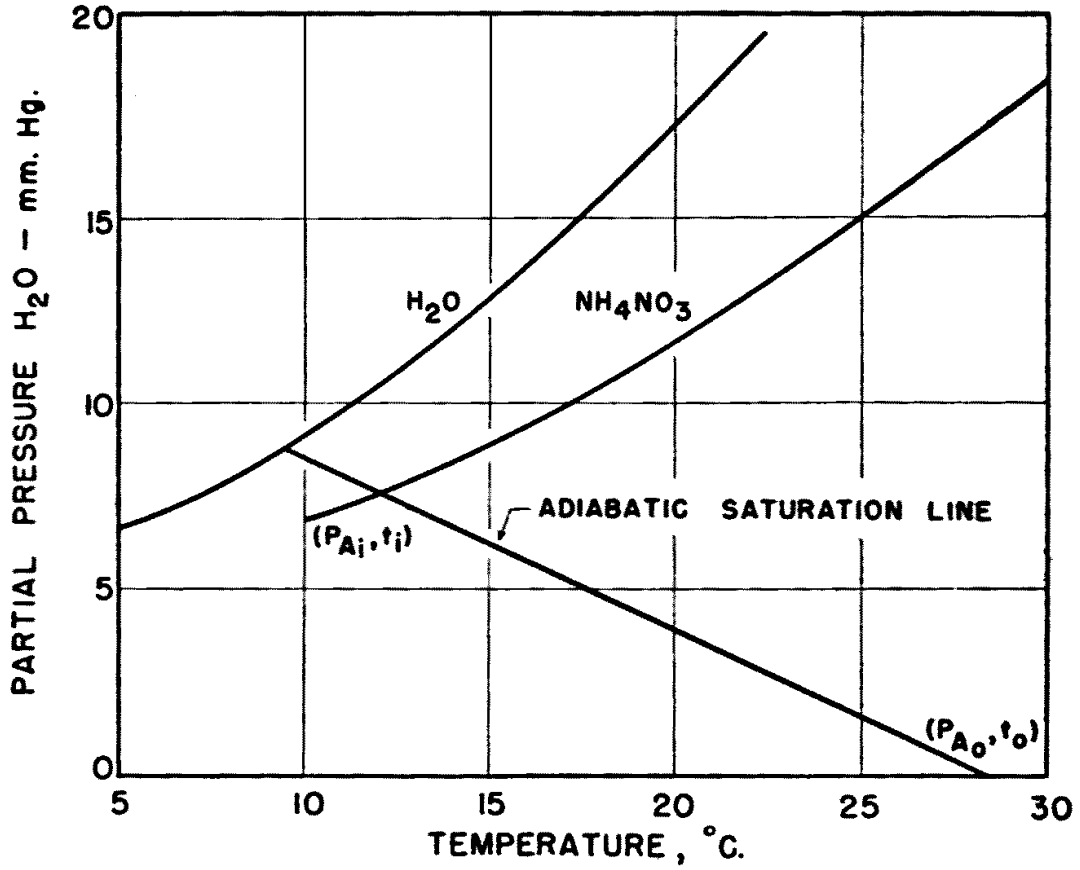

Figure 10.1.: Vapor pressure H_2O over water and saturated aqueous solutions of NH_4NO_3

10.2. Drying Drops in Still Dry Air with Heat of Cirystallization and Supersaturation Effects

Although the drying time of a one millimeter drop in room temperature air may be greater by a factor of approximately 10^3 than the drying time in usual 'spray-drying operation, the history of such a drop is of interest in predicting phenomena which might occur in the latter case.

Figure 10.2a through Figure 10.2d show D_p^2 and ΔT vs. time for the evaporation of drops which contained .dissolved and suspended materials, and were supported on a $1/2$-mil manganin-constantan thermoelement in the special dryer described previously. So long as the drops presented a completely wetted surface to the drying air, $\frac{dD_p^2}{d\tau}$ and ΔT are a measure of the drying rate at any time. During the falling-rate period, after a particle structure has been formed At may still be a measure of the rate of drying since it is a measure of heat transfer and consequently a measure of the rate of evaporation. Since the sequence of physical events is

complicated by heats of solution and crystallization, changes in specific gravity, changes in density, and shrinkage of particle structure, the interpretations below must be considered to be primarily qualitative. Figure 10.2a shows results for ,the drying of a drop containing 3×10^{-4} g of NH_4NO_3. The average concentration was controlled by drawing up a definite amount of standardized solution into the microburette and forcing it out onto a thermoelement ahead of excess solvent.
During the first period of drying up to the point of crystallization, $\frac{dD_p^2}{d\tau}$ and ΔT remain effectively constant as predicted. The gradual fall in Ai during the first period of drying was probably real even though the conduction effect of the thermoelement wires was more apparent as the drop diameter decreased. This increase in drop temperature can be attributed to an increasing concentration in the surface (supersaturation evidently occurred since crystals appeared suddenly, covering the surface completely), and to the effect of heat of solution which is appreciable for NH_4NO_3 (as the salt concentrated, heat was evolved, T_i rose and ΔT was no longer an exact measure of the evaporation rate). The rapid drop in ΔT and rise in T_i at about 600 s was due to a high heat of crystallization evolved at this point (approximately 20 % of the latent heat of evaporation of water). As soon as crystallization of the supersaturated solution in the surface was complete, a lowering of T_i again occurred because moisture was still being evaporated.
Figure 10.2b presents data for the drying of a drop containing 1.9×10^{-4} g of NaCl. Here supersaturation did not occur on the surface, but crystals appeared near the thermoelements as soon as those areas became sufficiently concentrated. Results show that the process exhibited a zone of decreasing ΔT, and a zone of constant ΔT, with $\frac{dD_p^2}{d\tau}$ constant throughout. As soon as a solid surface was formed, the drop temperature increased and ΔT fell rapidly. The zone of gradually decreasing ΔT may be interpreted in the same manner as the first period of drying of the drop described in the previous paragraph (the original value of ΔT can be estimated as in Figure 10.1); the zone of constant ΔT may be interpreted as a condition of quasi-thermal equilibrium caused by crystallization (the value of ΔT for this period can be estimated by drawing Equation 3.16 on Figure 10.1); the final zone, that of rapidly decreasing ΔT, was the falling-rate period.
Figure 10.2c concerns the drying of an aqueous drop of non-soluble, suspended green dye. Here ΔT was nearly that expected for a pure water drop since the drop contained an inert material which did not affect the vapor pressure. Under these circumstances the drying was simplified, except for a shrinkage of the solid particle during the falling-rate period. The transition between constant-rate and falling-rate period was not sharp largely because of the fact that the surface became dried first in patches near the points where transfer was greatest (around the thermoelement wires at the top of the drop), and the whole surface was not in the same period of drying at the same time.
Figure 10.2d shows data for the drying of a drop of reconstituted dried whole milk. Results are similar to Figure 10.2c, including shrinkage during the falling-rate

period. Again ΔT is nearly that for pure water because milk exhibits only a slight lowering of the vapor pressure of water.
Because actual spray particles are atomized to about one-tenth diameters of the suspended drops used in these tests and because actual ΔT's are on the order of ten times those used in these tests, the time of drying in spray drying will be of the order of 10^{-3} times the drying periods studied here. In so short a time the dynamic equilibrium for any one phase of drying may never be reached, and the physical picture represented by curves of the type shown in Figure 10.2a through Figure 10.2d will be slurred and smoothed into a continually changing form not amenable to analysis. However, these results demonstrate some of the factors involved.

10.3. Formation of Solid Surfaces

In the theoretical treatment, saturation considerations in the surface of an evaporating droplet were predicted, but no criterion was developed for the conditions necessary for crystallization. This omission can be filled by assuming that crystals appear at any point on the surface where the rate of accumulation of non-volatile material by evaporation exceeds the rate at which it diffuses into the center of the drop along concentration gradients. This assumption suggests the possibility that crystals can form before conditions for average saturation are reached and that crystals first form on the forward side of the drop, where the rate of evaporation is greatest. The same statements should apply for drops containing suspended solids, but in this case the meaning of saturation and diffusion cannot be clearly defined.
To support the expectation that solid surfaces form before the average drop concentration reaches the saturation value, it was noted during the evaporation tests on the constant diameter drops reported in Table 6 that small crystals appeared at the bottom of the drop containing 46 % NH_4NO_3 and that a crystal cap formed at the bottom of the drop containing 50 % NH_4NO_3. Saturation concentration for aqueous NH_4NO_3 solutions at 12 °C, the temperature of the drops, is approximately 61 %, which indicated a considerable concentration gradient existed from the surface of the drop into the interior.
This effect was even more striking in the case of a suspended drop of NH_4NO_3 solution evaporating in 210 °C air. The drop surface suddenly clouded with crystals after two seconds of evaporation when the diameter was 0.096 cm and the average salt concentration was of the order of 0.5 g of NH_4NO_3 to 1.0 g of water. The surface temperature at that time must have been considerably higher than 51 °C, which would be the surface temperature for a water drop under the same conditions. At 51 °C the concentration of NH_4NO_3 would have to be 3.5 g of salt to 1.0 g of water before crystals would appear. These crystals persisted for three more seconds up to a diameter of 0.090 cm at which time the temperature of the surface had increased to about 170 °C and the crystals melted. At 100 °C, the surface must have been

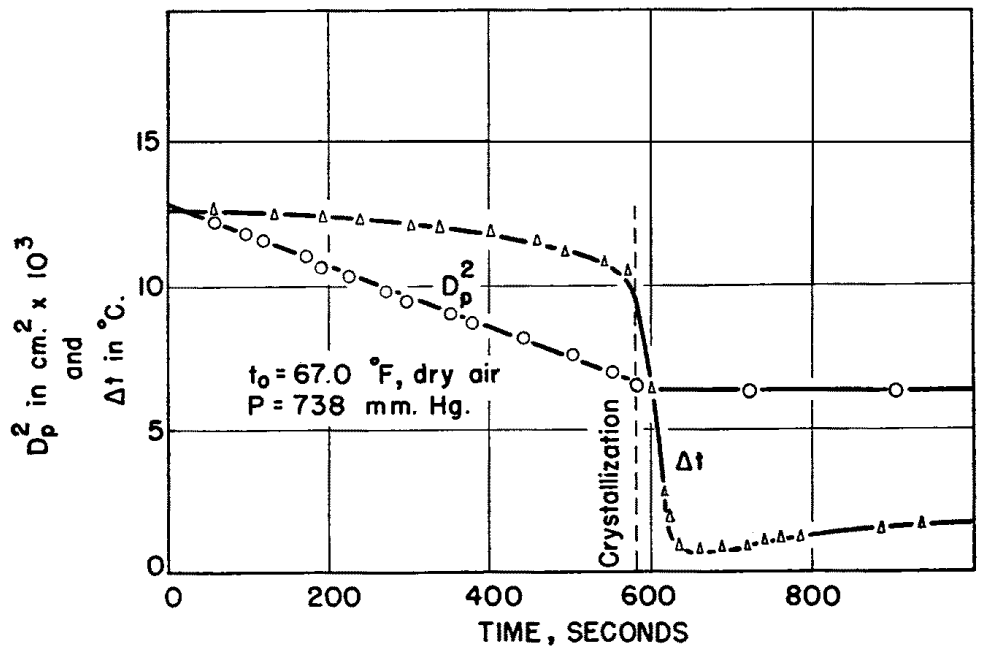

(a) D_p^2 and ΔT vs. time for drop containing NH_4NO_3 drying in still air

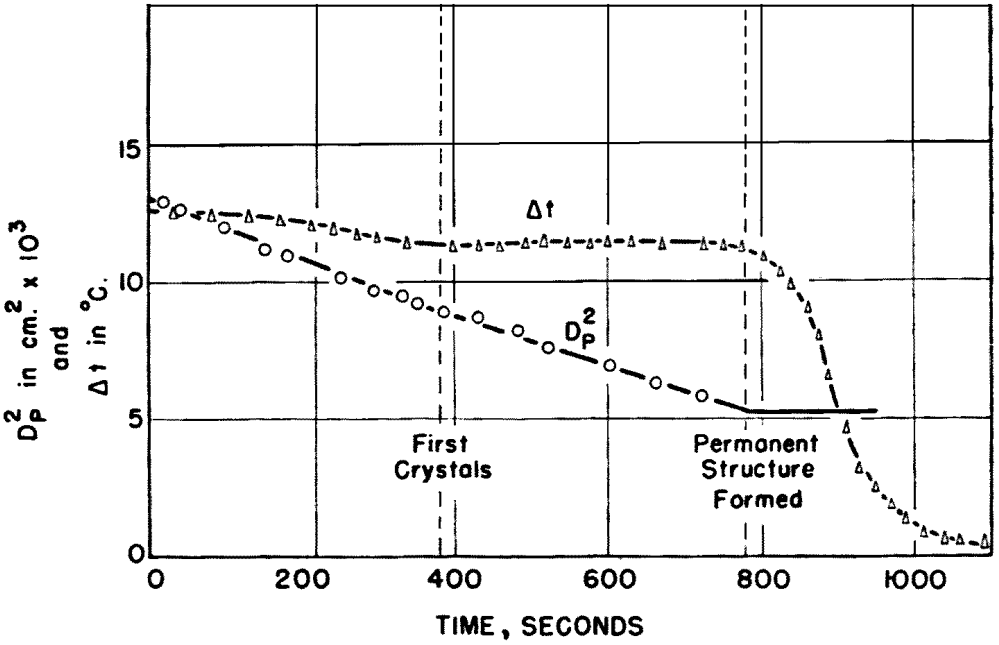

(b) D_p^2 and ΔT vs. time for drop containing 1.9×10^{-4} g NaCl drying in still air
$T_o = 20.4\,^\circ\mathrm{C}$
$P = 738\,\mathrm{mm\,Hg}$ (983.9 mbar)

Figure 10.2.: D_p^2 and ΔT vs. time for drop containing different substances

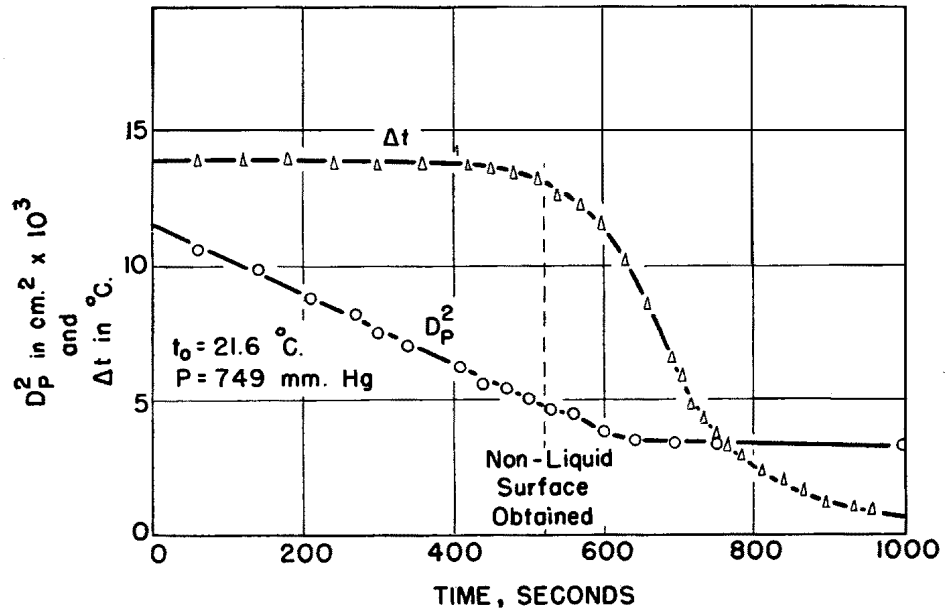

(c) D_p^2 and ΔT vs. time for drop containing MDD 1594 DuPont dye drying in still air

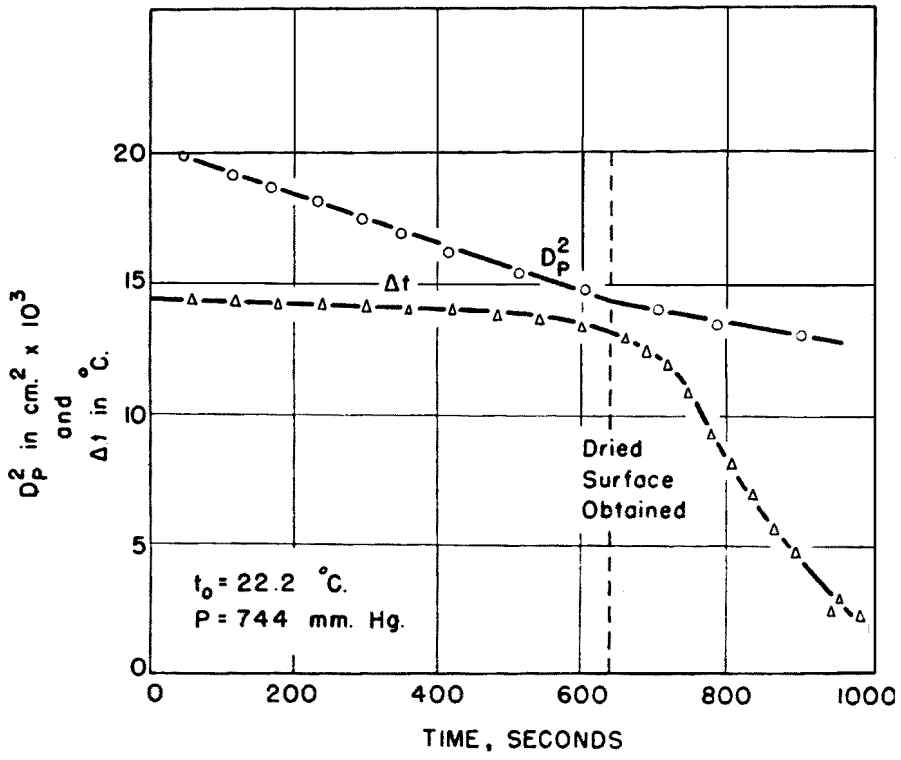

(d) D_p^2 and ΔT vs. time for drop containing reconstituted "klim" (dried whole milk) drying in still air

Supplementary Figure 10.2.: (Cont.)

supporting 8.7 g of salt to 1.0 g of water whereas the average concentration of the drop was considerably less than 3.0 g of salt to 1.0 g of water.

10.4. Qualitative Picture of Evaporation of a drop Containing Sodium Chloride

Starting at a diameter of nearly one millimeter and a concentration of approximately 20 % a drop containing sodium chloride evaporated as a pure liquid drop until cloudy crystals appeared on the side of the drop facing the oncoming air stream. This crystal cap grew rapidly until it covered the whole drop with shiny white crystals. No appreciable change in diameter occurred after the crystal cap covered the surface. The crystal surface soon lost some of its luster, and blowholes into the drop appeared at the downstream side. These holes were attributed to a vacuum created by the removal of dilute solution from the center, which was relieved by a blowhole through the particle's surface. The picture was the same whether the drop was evaporated in a 200 °C hot air stream or in room temperature still dry air, the only difference in the two processes being the time of evaporation, 20 s vs. 2000 s or 33.3 min.

11. Estimation of Drying Time

For most cases of the drying of a single aqueous spray droplet, the evaporation rate for the first period of drying can be computed from an equation for the rate of heat transfer

$$q_{ai} = hA \cdot (T_o - T_i) \tag{11.1}$$

for which the required heat-transfer coefficient, h, for situations where radiation transfer is negligible, may be estimated from the relation

$$h = h_c = \frac{\kappa}{D_p} \cdot \left(2.0 + 0.54\,\mathrm{Re}^{\frac{1}{2}}\right) \tag{11.2}$$

where Equation 11.2 is restricted to aqueous drops.
The drop temperature, T_i, can be estimated from a psychrometric chart at the point where the adiabatic saturation line drawn through the drying air conditions crosses the curve for humidity over a saturated solution of the nonvolatile material (Figure 10.1). If the non-volatile material is in suspension without influencing the vapor pressure, the drop or surface temperature can be approximated by the temperature of adiabatic saturation in the case of water, or by the normal wet-bulb temperature in the case of liquids other .than water. If crystallization is taking place, T_i may be estimated by a wet-bulb temperature given by Equation (15).
In applications to spray drying where atomization produces drop diameters of 100 µm and essentially concurrent operation occurs, a further and conservative simplification can be made by using the limiting value of $\frac{h_c D_p}{\kappa} = 2.0$ at $\mathrm{Re} = 0$.
The first period of drying ends when the liquid surface of the drop becomes a solid surface. This may occur before conditions of uniform saturation throughout the drop are reached, and may result in a final particle of unusual porosity. Critical average moisture contents calculated from the data of Figure 10.2a through Figure 10.2d are too meager to have meaning. Theoretical calculations of the time and average moisture content when internal liquid concentration gradients can no longer move the solute flux can be made but are so complex that they are of little practical use. It can be shown from the heat balance on a drop with inert solids in suspension that during the falling-rate period the drying rate still may be estimated by Equation 11.1 if the proper average temperature difference can be determined. Thus, a heat balance for drying in still air gives the following expression for the falling rate:

$$\frac{\mathrm{d}W}{\mathrm{d}\tau} = \frac{6h}{\lambda D_{pc} \rho_s} (\Delta T) + \frac{C_s}{\lambda} \cdot \frac{\mathrm{d}\,(\Delta T)}{\mathrm{d}\tau} \tag{11.3}$$

where now ΔT is a variable, as shown in Figure 10.2a through 15d. Using the data of Figure 10.2c, it was calculated that down to a ΔT of 1 °C, the second term of the right side of Equation 11.3 accounts for only about 3 % of the heat transferred. The same condition holds true for practical spray-drying operations. Thus, it might be concluded that for materials which do not crystallize from solution to give extraneous heat effects, the falling rate drying time for drops may be estimated by the expression

$$(\tau_2 - \tau_c) = \frac{\lambda D_{pc} \rho_s}{6h} \cdot \frac{(W_c - W_2)}{\Delta T_{\text{avg}}} \tag{11.4}$$

where ΔT_{avg} is a proper time average. In addition to the usual problem of specifying the proper critical moisture content, W_c, it is also necessary to know the value of D_p at W_c. Thus, an approximation for total drying time Θ at low Reynolds number for drops containing undissolved solids may be written as

$$\Theta = \frac{\lambda_i \rho_l \cdot \left[D_{p1}^2 - D_{pc}^2\right]}{8\kappa \cdot (T_o - T_i)} + \frac{\lambda \cdot (W_c - W_2)\, \rho_s D_{pc}^2}{12\kappa \Delta T_{\text{avg}}} \tag{11.5}$$

in terms of: original atomized diameter, D_{p1}; final particle diameter, D_{pc}; critical moisture content, W_c; final moisture content, W_2; final particle density, ρ_s; and the physical properties of the components of the system. Use of Equation 11.5 implies a knowledge of a relationship between moisture content and temperature. From the temperature data of Figure 10.2c and Figure 10.2d, it appears that a logarithmic mean average temperature is a fair approximation of ΔT_{avg} as far as the ΔT curve goes since for the purpose of calculating drying time the curve may be characterized as an exponential decay curve. Such an assumption, which allows a slower rate of drying the lower the moisture content, is exactly equivalent to the usual assumption made in drying calculations that the rate of drying is proportional to moisture content when the drying air conditions remain constant. For spray drying in high temperature air with essentially concurrent operation, it is a well-known fact that the air temperature falls much more rapidly than the particle temperature increases. In Equation 11.5 this effect must be taken into consideration for an average $(T_o - T_i)$ during the constant-rate period and for a logarithmic mean average of the temperature difference during the falling rate period.

12. Acknowledgement

The authors wish to acknowledge the Procter and Gamble Co. and the Wisconsin Alumni Research Foundation for financial assistance, and Prof. O. A. Hougen for suggestions.

A. Biographical Notes

A.1. William E. Ranz (1922–2009)

Ranz, William E. 87, of Edina, MN, passed from this life on October 20, 2009. He was born in Blue Ash, OH where he grew up. A decorated WWII veteran, he graduated from the University of Cincinnati, and later he received MS and Phd degrees in Chemical Engineering from the University of Wisconsin - Madison.
After working at the University of Illinois, Cambridge University – England and Pennsylvania State University, William became a long-time member (1952–1992) of the faculty of the Department of Chemical Engineering at the University of Minnesota. He enjoyed his work immensely, especially the interaction with both undergraduate and graduate students.
In 1965 he was recognized with a University of Minnesota Distinguished Teaching Award. His students often honored him as a tough, but enjoyable, part of their march to graduation in annual Senior Banquet skits. He enjoyed roasting them in return.
After retiring, William enjoyed traveling with his wife Virginia throughout the world and visiting his children and expanding bunch of grandchildren. William is survived by his loving wife of 35 years, Virginia, his children and their families Beth Ranz Riggs of Miles City, MT, Christina Ranz Cavin of South Burlington, VT, Roger A. Ranz of Shelburne, VT and Jennifer Ranz of Greensboro, VT, his sisters-in-law, nieces and grandnieces in Minnesota, Ohio and beyond.

A.2. W. Robert Marshall (1916–1988)

W. Robert Marshall, former dean of the College of Engineering of the University of Wisconsin, died at age seventy-one on January 14, 1988, after suffering a heart attack. At the time of his death he was still quite active professionally and was serving as the director of the University-Industry Research Program. This influential position was a fitting capstone to an impressive career, which included teaching, research, industrial consulting, professional society leadership, and university administration. He spent much of his time at the University of Wisconsin trying to strengthen ties between academia and industry. He was also an effective author, whose books and writings strongly influenced chemical engineering education and research.
Bob Marshall was born on May 19, 1916, in Calgary, Alberta, and came to the

United States as a child; he became a naturalized U.S. citizen on March 20, 1944. He was an undergraduate in chemical engineering at Armour Institute of Technology (now called Illinois Institute of Technology), which awarded him the B.S. in 1938. In the spring of 1937 Professor Olaf A. Hougen of the University of Wisconsin was a visiting professor at Armour, and forged a lifelong relationship with Bob, who accompanied Olaf back to Madison for graduate study. In 1941 he received the Ph.D. from the University of Wisconsin based on a thesis entitled "Through-Circulation Drying" done under Professor Hougen's direction.

In 1941 Bob accepted a position in the Engineering Department of the Engineering Experiment Station of the E.I. du Pont de Nemours and Company in Wilmington, Delaware. The du Pont experience played an important role in shaping Bob's professional attitudes – in particular his emphasis on solving real engineering problems, his feeling that science and engineering are equal partners in the advancement of technology, and his concern that research results should be put in such a form that they will be of direct use to the practicing engineer.

During his stay at du Pont Bob served as an instructor in the evening program of the Extension Division of the University of Delaware. This led to his collaboration with Professor Robert L. Pigford on the book *The Application of Differential Equations to Chemical Engineering Problems*, which was published in 1947 by University of Delaware Press. This book was extremely influential because it was richly illustrated with imaginative and important problems, many of which even today provide excellent examples of how mathematics can be used to solve problems of engineering interest.

In 1947 he was once again attracted to the University of Wisconsin by Olaf Hougen, where he was given an appointment as associate professor of chemical engineering. His teaching activities included a new graduate course on applied mathematics (based on his book) and the graduate course on mass-transfer operations, which he revitalized by introducing new ideas based on transport phenomena and boundary-layer theory. His research program took shape quickly, and he soon had a rather large graduate group working on a wide variety of drying processes. He and his students made major contributions, particularly in the areas of atomization and spray drying, and for some time he was referred to as "the founder of modern spray-drying technology." All in all Bob directed the Ph.D. theses of thirty-two graduate students, most of whom have made substantial professional contributions.

In 1954 his famous monograph *Atomization and Spray Drying* appeared as the second volume of the Chemical Engineering Progress Monograph Series, published by the American Institute of Chemical Engineers. This monograph summarized his seven years of research at du Pont and six years of research with his students at the University of Wisconsin. In this book Bob showed how applied mathematics, fluid dynamics, transport phenomena, statistics, and physical chemistry could be used to solve critical problems in spray processing, and that this could be done in such a way as to obtain workable design methods and performance characteristics of spray dryers. In 1981 a practicing engineer in a large U.S. industry said of

Bob's monograph, "Using many of the principles described in this publication, we have improved equipment capacity nearly tenfold with accompanying major improvements in costs. When you consider that we produce approximately two billion pounds of spray-dryed products annually, these improvements were and are of obvious economic value." Bob was an early practitioner of "engineering science" in the best sense of that term. His work was the basis of industrial processes that were to produce billions of pounds of products every year.

Although Bob was a gifted teacher and a brilliant research supervisor, he was soon asked to transfer his talents to help solve administrative problems. In 1953 he was appointed associate dean of the College of Engineering and executive director of the Engineering Experiment Station. In this capacity Bob was able to combine his originality and enthusiasm to bring about a number of changes. He chaired the committee that led to the establishment of the Department of Nuclear Engineering, which included both graduate and undergraduate programs. Along with Farrington Daniels he established the Solar Energy Laboratory. He was also instrumental in the development of the Materials Science Program. He was directly responsible for setting up a lively exchange program with Monterrey Institute of Technology in Mexico, and also a student exchange between the University of Wisconsin and universities in West Germany.

In 1971 Bob was named dean of the College of Engineering, a post that he was to hold for ten years. In this position he was able to continue being creative in an administrative way. His strong belief that engineering opportunities should be open to women and minorities led to the creation of one of the first student programs for minorities in engineering in the country. He also encouraged the involvement of College of Engineering faculty members in the Development Program for the Institute of Technology at Surabaya in Indonesia; this involved the building of a new campus and providing postgraduate training for the engineering faculty. His concern for the inability of engineers to be effective in the political and public service arenas led him to establishing courses in the General Engineering Department dealing with the interaction of engineering and society. He also gave positive encouragement to the development of the first instructional program on technical Japanese translation in the United States, and set up a mechanism for faculty and student exchange between the chemical engineering departments of the University of Wisconsin and Kyoto University.

After retiring from the deanship in 1981, Bob accepted the assignment of director of the University-Industry Research Program. In this capacity he found new opportunities to put his experience and leadership to work by facilitating and supporting faculty research relationships with industry. Bob concerned himself with the diversity of research activities on the entire campus and the possible beneficiaries of this research throughout the state. He worked on such problems as patent advice for professors, small business development, and sources of external research support.

Bob Marshall was an enthusiastic supporter of the American Institute of Chemical

Engineers (AIChE) and had a keen sense of responsibility to the organization. He accepted numerous committee assignments and was the primary force in establishing the Continuing Education Committee, which he chaired from 1964 to 1967. He served as director from 1956 to 1958, vice-president in 1962, president in 1963, past president in 1964, and treasurer from 1976 to 1980. The institute recognized his research and leadership roles by bestowing on him many awards and special recognitions: Institute Lecturer in 1952, William H. Walker Award in 1953, Professional Progress Award in Chemical Engineering in 1959, and Founders Award in 1973. In 1983, on the occasion of the Diamond Jubilee of the AIChE, he was included in the list of thirty "Eminent Chemical Engineers" in the United States.

In addition to participation in the AIChE, Bob also served on seven committees of the American Society for Engineering Education, including the Black Engineering Colleges Development Committee and the Professional Development Committee of the Biomedical Engineering Division. For Argonne National Laboratory he served as chairman of the Chemical Engineering Review Committee and as member of the Policy Advisory Board. He was very active in the Associated Midwest Universities organization, serving on the board of directors and as vice-president in 1961 and 1962 and as president in 1962 and 1963. He had a three-term stint on the Executive Committee of the Engineers Joint Council and served for two years as vice-president of that organization.

In addition to the awards he received from the AIChE, Bob Marshall was accorded many other honors, including fellow of the American Academy of Arts and Sciences in 1960, the Gold Medal of the Verein Deutscher Ingenieure in 1974, and an honorary doctor of laws from the Illinois Institute of Technology in 1981. From his own College of Engineering he received the Ragnar E. Onstad Award for Service to Society in 1981, and the Byron Bird Award for Excellence of a Research Publication in 1983.

Election to the National Academy of Engineering (NAE) came in 1967. Within the NAE he served on the Commission on Education, of which he was vice-chairman in 1969 and chairman from 1970 to 1974. He also was a member of the Committee on the Interplay of Engineering with Biology and Medicine from 1968 to 1973, and served as chairman from 1969 to 1973. In addition he was on the Committee on Membership from 1968 to 1970.

Bob was always professional and gentlemanly. He was devoted to providing the best possible opportunity for his colleagues and students to deploy their talents and energies to maximum effectiveness. It came naturally to him to convey to others his enthusiasm for their skills and potential, and he provided them with the chance to present their ideas and hopes in a supportive setting. He never assumed any credit for their contributions. He simply wanted his associates to be able to attain their goals. Many people owe their own professional success to words of encouragement from Bob Marshall. He was always available to his friends and colleagues when they needed help or advice.

In addition to his university and professional activities, Bob found the time to support the community in which he lived. He was a member of the school board in Monona, Wisconsin, for six years. He was vice-president of the Madison Downtown Rotary Club from 1984 to 1985, and he served as a member of the board of directors of United Way from 1981 to 1982.
Bob was a very genuine and modest person, and despite his exalted standing in the professional world, he was never ostentatious or condescending. He always gave his very best efforts to every task that he undertook; but he did more than that – his performances always had a sense of "style" and "flair" that few others can attain. Whether he was chairing a committee, making a technical presentation, or giving a eulogy at a memorial service, Bob could supply a little extra spirit or warmth or humor that would upgrade the performance from excellent to superb. He left his colleagues, friends, and family a remarkable legacy of accomplishments, inspiration, and high principles.

Bibliography

[1] J. R. Adams and A. R. Merz. Hygroscopicity of Fertilizer Materials and Mixtures. *Industrial and Engineering Chemistry*, 21(4):305–307, 1929.

[2] J. A. Bearden. A Precision Determination of the Viscosity of Air. *Physical Review*, 56(10):1023, 1939.

[3] S. Chapman and T. G. Cowling. *The Mathematical Theory of Non-uniform Gases*. Cambridge University Pree, New York, 1 edition, 1939.

[4] T. H. Chilton and A. P. Colburn. Mass Transfer (Absorption) Coefficients Prediction from Data on Heat Transfer and Fluid Friction. *Industrial and Engineering Chemistry*, 26(11):1183–1187, 1934.

[5] A. P. Colburn. A Method of Correlating Forced Convection Heat Transfer Data and a Comparison with Fluid Friction. *Transactions of the American Institute of Chemical Engineers*, 29:174–210, 1933.

[6] A. P. Colburn and R. L. Pigford. *General Theory of Diffusional Operations*. McGraw-Hill Book Co., Inc., New York, 3 edition, 1950.

[7] C. F. Curtiss and J. O. Hirschfelder. Thermodynamic Properties of Air. I. Technical Report CM-472, Wisconsin University, Madison, 1948.

[8] C. F. Curtiss and J. O. Hirschfelder. Thermodynamic Properties of Air. II. Technical Report CM-518, Wisconsin University, Madison, 1948.

[9] W. Elenbaas. The dissipation of heat by free convection of spheres and horizontal cylinders. *Physica*, 9(3):285–296, 1942.

[10] W. Frössling. Über die Verdunstung fallender Tropfen. *Gerlands Beiträge zur Geophysik*, 52:170–216, 1938.

[11] N. Fuchs. Über die Verdampfungsgeschwindigkeit kleiner Tröpfchen in einer Gasatmosphäre. *Physikalische Zeitschrift der Sowjetunion*, 6:224–243, 1934. available in translation "*Concerning the velocity of Evaporation of small Droplets in a Gas Atmsphere*" as *Techn. Mem.* 1160, *Nat. Advisory Comm. Aeronaut.*

[12] J. O. Hirschfelder, R. B. Bird, and E. L. Spotz. The Transport Properties for Non-Polar Gases. *Journal of Chemical Physics*, 16(10):968–981, 1948.

[13] J. O. Hirschfelder, R. B. Bird, and E. L. Spotz. The transport properties of gases and gaseous mixtures. II. *Chemical Review*, 44(1):205–231, 1949.

[14] J. O. Hirschfelder, R. B. Bird, and E. L. Spotz. Viscosity and Other Physical Properties of Gases and Gas Mixtures. *Transactions of the American Institute of Mechanical Engineers*, 71:921–937, 1949.

[15] H. L. Johnston and K. E. McCloskey. Viscosities of Several Common Gases between 90°K and Room Temperature. *Journal of Physical Chemistry*, 44(9):1038–1058, 1940.

[16] H. F. Johnstone and R. V. Kleinschmidt. The Absorption of Gases in Wet Cyclone Scrubbers. *Transactions of the American Institute of Chemical Engineers*, 34:181–198, 1938.

[17] H. F. Johnstone, R. L. Pigford, and J. H. Chapin. Heat transfer to clouds of falling particles. *University of Illinois Engineering Experiment Station Bulletin Series*, 330, 1941.

[18] H. F. Johnstone, R. L. Pigford, and J. H. Chapin. Heat Transfer to Clouds of falling Particles. *Transactions of the American Institute of Chemical Engineers*, 37:95–133, 1941.

[19] L. V. King. XII. On the convection of heat from small cylinders in a stream of fluid: Determination of the convection constants of small platinum wires with applications to hot-wire anemometry. *Philosophical Transactions of the Royal Society A*, 214(509–522):373–432, 1914.

[20] H. Kramers. Heat transfer from spheres to flowing media. *Physica*, 12:61–81, 1946.

[21] I. Langmuir. The Evaporation of Small Spheres. *Physical Review*, 12(5):368, 1918.

[22] H. Mache and A. Hebra. Zur Messung der Verbrennungsgeschwindigkeit explosiver Gasgemische. *Sitzungsberichte / Akademie der Wissenschaften in Wien, Philosophisch-Historische Klasse, Abt.IIa*, 150:157–174, 1941.

[23] E. Mack. Average Cross-Sectional Areas of Molecules by Gaseous Diffusion Methods. *Journal of the American Chemical Society*, 47(10):2468–2482, 1925.

[24] D. S. Maisel and T. K. Sherwood. Evaporation of Liquids into Turbulent Gas Streams. *Chemical Engineering Progress*, 46:131–139, 1950.

[25] W. H. McAdams. *Heat Transmission*. McGraw-Hill Book Co., Inc., New-York, 2 edition, 1942.

[26] P. Meyer. Heat transfer to small particles by natural convection. *Transactions of the Institute of Chemical Engineers*, 15:127–131, 1937.

[27] H. W. Morse. On Evaporation from the Surface of a Solid Sphere. Preliminary Note. *Proceedings of the American Academy of Arts and Sciences*, 45(14):363–367, 1910.

[28] R. Schirmer. Die Diffusionszahl von Wasserdampf-Luft-Gemischen und die Verdampfungsgeschwindigkeit. *Zeitschrift des Vereins deutscher Ingenieure Beihefte Verfahrenstechnik*, 82(6):170–177, 1938.

[29] T. K. Sherwood and Williams G. C. Evaporation of falling drops. Technical Report 6538, Natl. Defence Res. Comm. Prog. Rep, 1941.

[30] W. J. Taylor and H. L. Johnston. An Improved Hot Wire Cell for Accurate Measurements of Thermal Conductivities of Gases over a Wide Temperature Range Results with Air between 87° and 375°K. *Journal of Chemical Physics*, 14(4):219–233, 1946.

[31] D. W. Van Krevelen and P. J. Hoftijzer. Drying of granulated materials. Part I. Drying of a single granule. *Journal of the Society of Chemical Industry*, 68(2):59–66, 1949.

[32] V. Vasilesco. Recherches expérimentales sur la viscosité des gaz aux températures élevées. *Annales de Physique*, 20:292–334, 1945.

[33] G. C. Williams and R. O. Schmitt. Humidity Measurements in Presence of Water-Soluble Salts. *Industrial and Engineering Chemistry*, 38(9):967–974, 1946.

[34] A. Winkelmann. Über die Diffusion von Gasen und Dämpfen. *Annalen der Physik*, 22(5):1–31, 1884.

[35] A. Winkelmann. Über die Verdampfung von den einzelnen Theilen einer kreisförmigen freien Oberfläche. *Annalen der Physik*, 35(11):410–429, 1888.

[36] A. Winkelmann. Über den Einfluss der Temperatur auf die Verdampfung und auf die Diffusion von Dämpfen. *Annalen der Physik*, 36(1):93–114, 1889.

[37] E. G. Zak. *Referativnyi Zhurnal, Geofizika*, 6:452, 1936.